STRONG OPTICAL SCATTERING BY FEMTOSECOND LASER INDUCED MICROBUBBLES INSIDE WATER AND OTHER MICROSCOPIC OBSERVATIONS

SAYED AHMED ISLAM SANNY

FACULTY OF SCIENCE
UNIVERSITY OF MALAYA
KUALA LUMPUR

2018

STRONG OPTICAL SCATTERING BY FEMTOSECOND LASER INDUCED MICROBUBBLES INSIDE WATER AND OTHER MICROSCOPIC OBSERVATIONS

SAYED AHMED ISLAM SANNY

THESIS SUBMITTED IN FULFILMENT OF THE REQUIREMENTS FOR THE DEGREE OF MASTER

DEPARTMENT OF PHYSICS
FACULTY OF SCIENCE
UNIVERSITY OF MALAYA
KUALA LUMPUR

2018

UNIVERSITY OF MALAYA

ORIGINAL LITERARY WORK DECLARATION

Name of Candidate: **SAYED AHMED ISLAM SANNY**

Matric No: **SGR150052**

Name of Degree: **MASTER OF SCIENCE**

Title of Project Thesis ("this Work"):

STRONG OPTICAL SCATTERING BY FEMTOSECOND LASER INDUCED MICROBUBBLES INSIDE WATER AND OTHER MICROSCOPIC OBSERVATIONS

Field of Study: **EXPERIMENTAL PHYSICS**

I do solemnly and sincerely declare that:

(1) I am the sole author/writer of this Work;
(2) This Work is original;
(3) Any use of any work in which copyright exists was done by way of fair dealing and for permitted purposes and any excerpt or extract from, or reference to or reproduction of any copyright work has been disclosed expressly and sufficiently and the title of the Work and its authorship have been acknowledged in this Work;
(4) I do not have any actual knowledge nor do I ought reasonably to know that the making of this work constitutes an infringement of any copyright work;
(5) I hereby assign all and every rights in the copyright to this Work to the University of Malaya ("UM"), who henceforth shall be owner of the copyright in this Work and that any reproduction or use in any form or by any means whatsoever is prohibited without the written consent of UM having been first had and obtained;
(6) I am fully aware that if in the course of making this Work I have infringed any copyright whether intentionally or otherwise, I may be subject to legal action or any other action as may be determined by UM.

Candidate's Signature Date:

Subscribed and solemnly declared before,

Witness's Signature Date:

Name:

Designation:

STRONG OPTICAL SCATTERING BY FEMTOSECOND LASER INDUCED MICROBUBBLES INSIDE WATER AND OTHER MICROSCOPIC OBSERVATIONS

ABSTRACT

Nonlinear interactions of focused femtosecond laser with water can provide interesting optical phenomena, most commonly, laser induced breakdown in water which creates plasma, self-focusing or filamentation because of loose geometrical focusing condition, white light generation and blue shifted by plasma, conical emission and associated spectra, as well as creation of optical cavitation bubbles and their motions inside water. However, in our work, in addition to the well-known phenomena we have observed a new kind of colorful optical scattering flash from femtosecond laser induced microbubble surface. A closer look under the microscopic observation of the focused region of femtosecond laser pulse leads us to observe this scattering. Additionally, in this work, we also have discussed the nonlinear optical process including our new finding phenomena to elucidate the underlying physical mechanisms and laser induced bubble mechanism from the micro level observational point of view.

Keywords: Laser, femtosecond, LIB, Microbubbles, Scattering, Optics

KUAT OPTIK BERSELERAK OLEH FEMTOSECOND LASER TERINDUKSI MICROBUBBLES DI DALAM AIR AIR DAN LAIN MICROSCOPIC PEMERHATIAN

ABSTRAK

Interaksi tak linear antara laser femtosecond dengan air membawa kepada fenomena optik yang menarik, di mana fenomena yang paling kerap merangkumi pecahan teraruh laser dalam air yang membawa kepada kewujudan plasma, fokus diri ataupun filamentasi yang disebabkan oleh keadaan geometri fokus yang longgar, penjanaan cahaya putih dan peralihan biru oleh plasma, pelepasan konikal dan spektrum yang berkaitan, serta penghasilan gelembung peronggaan optik dan gerakan mereka dalam air. Dalam kajian ini, selain daripada semua fenomena terkenal yang disebut, kami telah memerhati suatu penyerakan optik yang berwarna-warni pada permukaan gelembung mikro yang disebabkan oleh laser femtosecond. Pemerhatian kawasan fokus laser femtosecond yang lebih teliti di bawah mikroskop membawa kami kepada penemuan fenomena penyerakan tersebut. Di samping itu, dalam kajian ini, kami juga membincangkan proses optik tak linear selain daripada fenomena baru yang disebut tadi untuk menjelaskan mekanisme-mekanisme fizikal asas di belakang fenomena itu serta mekanisme gelembung teraruh laser daripada sudut penglihatan pemerhatian pada tahap mikro.

Kata kunci: Laser, femtosecond, LIB, Scattering, Optik

ACKNOWLEDGEMENTS

This work would not have been possible without supports and encouragement from a number of peoples. My foremost and greatest thanks go to my research supervisor Professor Dr. C. H. Raymond Ooi. His wise and thoughtful advice guided me to achieve a novel finding from my research. I would also like to thank our research group Quantum and Laser Science at the University of Malaya, it is a great experience to be a part of this group. My deep acknowledgment will go to all of my colleagues of this research group for creating such a friendly environment so that I was able to complete my work in time. I would like to give a spatial thank to Loh Wai Ming for his support in my all critical moments, besides I am also remembering other colleagues names Nadi, Davud, Faisal for being as like family.

I would like to University of Malaya because of making opportunity for me to study in this university and arranging the financial supports by High Research Impact grant. Also, thanks to the administration of Department of Physics and Faculty of Science, and those who were my examiner and panel members to evaluate my work.

My ultimate thanks and love to go my parents and my younger sister, they are my first pure well-wisher and encouraged to acquire knowledge and supporting me from my back. Also, I am thanking my other close relatives and friends, those helped me to overcome problems whenever I faced.

TABLE OF CONTENTS

ABSTRCT ..... **iii**

ABSTRAK ..... **iv**

ACKNOLEDGEMENTS ..... **v**

TABLE OF CONTENTS ..... **vi**

LIST OF FIGURES ..... **viii**

LIST OF TABLES ..... **x**

LIST OF SYMBOLS AND ABBREVIATIONS ..... **xi**

LIFT OF APPENDICES ..... **xii**

CHAPTER 1: INTRODUCTION **1**

1.1 Introductory 1

1.2 Literature Review 2

1.3 Objectives 5

1.4 Outline 5

CHAPTER 2: CONCEPT OF LASER **6**

2.1 Laser Fundamentals 6

2.2 Device Types of Laser: CW and Pulse Laser and Some Quantities 9

2.3 The Femtosecond Laser and Pulse Generation 11

CHAPTER 3: REVIEW ON LASER WATER INTERACTION **18**

3.1 Creation of Plasma, Optical Breakdown and Filamentation 18

3.2 Optical Cavitation Bubbles 23

3.3 White Light Continuum Generation and Conical Emission 24

CHAPTER 4: EXPERIMENTAL PROCEDURE 27

4.1 Experimental Setup Model 27

4.2 Equipment Description and their uses 29

CHAPTER 5: INVESTIGATED RESULT AND DISCUSSION 31

5.1 Laser Induced Breakdown in Water and Filamentation 33

5.2 Colors and Blue Shift by Plasma and White Light Spectra 34

5.3 Creation of Bubbles 38

5.4 Rapid Generation of Bubbles 39

5.5 Colored Light Scattering by Bubbles 41

5.6 Approximate Position and Size Distribution of Scattering Color Bubbles 50

5.7 Laser Power and Related Effects on Multi Spectral Colors 58

5.8 The Forces on Bubbles 59

CHAPTER 6: CONCLUSION AND SCOPE OF FUTURE WORK 65

REFERNCES 68

LIST OF PUBLICATIONS AND PAPERS PRESENTED 76

APPENDICES 77

LIST OF FIGURES

Figure 1.1 :	Phenomena and findings when high intense femtosecond laser focused inside water. …….	4
Figure 2.1 :	Laser and characteristics of lasers (Herd et al., 1997). …….	6
Figure 2.2 :	Laser devices. ……...	7
Figure 2.3 :	(a) CW laser and pulsed laser & (b) Laser quantity. …….	9
Figure 2.4 :	Chirped Pulse Amplifier (CPA). ……..	12
Figure 2.5 :	A schematic diagram of a stretcher (Backus et al., 1998). ...	14
Figure 2.6 :	A schematic diagram of a stretcher (Backus et al., 1998). ...	15
Figure 2.7 :	Two schematic diagram of amplifiers (a) Regenerative amplifier & (b) Multipass amplifier (Cheriaux & Chambaret, 2001) …….	16
Figure 2.8 :	Schematic diagram for pulse compressor (Backuset el al., 1998). ……	17
Figure 4.1 :	Schematic diagram of experimental Setup. ……...	28
Figure 4.2 :	Current VS Power Curve. ……..	29
Figure 5.1 :	Twinkling color lights without halogen light. ……	32
Figure 5.2 :	Twinkling color lights with halogen light. …….	32
Figure 5.3 :	Laser induced breakdown in water and filamentation. ……...	33
Figure 5.4 :	Spectroscopic graphs of laser induced plasma inside water…	36
Figure 5.5 :	Generation of bubbles (side view) for different laser intensity. ……	40
Figure 5.6 :	Sparkling color lights and dark bubbles. ……	42
Figure 5.7 :	Color light scattering by single bubbles. ……	43
Figure 5.8 :	Multi filaments by focused femtosecond laser in air. ……	44
Figure 5.9 :	Multi filaments by focused femtosecond laser in air. …….	45
Figure 5.10 :	Bubbles movement and scattering of color light within 0.48 second. ……..	45
Figure 5.11 :	Position distribution during brightest spark……	51

Figure 5.12 : Bubble diameter and color distribution. …… 54

Figure 5.13 : Scatter plot of the spatial distributions of the sparkling colors. …… 56

Figure 5.14 : Distributions of the bubble diameters for each color. …… 57

Figure 5.15 : Overall distribution of bubbles with all colors and a Gaussian fit. …….. 57

Figure 5.16 : Impact of laser power and frequency. …… 58

Figure 5.17 : Unfocused color and vibrant motion. …… 31

LIST OF TABLES

Table 2.1 : Commercial Lasers. …….. 10

Table 1.1 : Scattering color and bubble diameter size distribution from different video clips. …….. 53

LIST OF SYMBOLS AND ABBREVIATIONS

LIB	:	Laser Induced Bubbles
RRB	:	Rapidly Running Bubbles
VBB	:	Violently Boiling Bubbles
NTU	:	Nephelometric Turbidity Units

LIST OF APPENDICES

Appendix A : Mathematical Expression for LIB . ……..…….. 77

Appendix B : Motional Direction of LIB……...…….. 80

Appendix C : Water Specification……... 82

CHAPTER 1: INTRODUCTION

In this chapter the literature review will be first discussed, forwarded by a short introductory, the objective of this work and finally outline of this thesis.

1.1 Introductory

Lasers are used to produce coherent beam of monochromatic light with high directional and relatively small divergence. In a coherent beam, all the photons are in the same phase, so it gives a single-color light and it is called monochromatic (where monochromatic means single wavelength of light). Although laser light is not found in nature, it is very important due to its many useful and practical applications. Those applications are designed based on laser matter interactions.

In terms of laser matter interaction, the physical outcomes are determined by the way photon energy is transferred into the target matters. At present, two type of most common laser systems are used for laser matter-interactions applications. First, Continuous Wave or CW Lasers. This class of laser continuously pumps and emits light. Secondly, Pulsed Laser. This class do not emit light continuously, but it emits in the form of an optical pulse. Following, the invention of laser technology, a large number of researcher and research groups across the world have been working to understand the behavior of matter as interact with both classes of laser. More recently, ultrafast laser processing is becoming a more reliable tool for practical and industrial applications due to their unique features and have opened exciting research opportunities in the field of laser-matter interaction. These following consequences motivated us to explore on the topic femtosecond laser water interaction where less investigation has been done. In our research we used regular water because of its essentiality of sustaining life and necessity of vast area of uses.

1.2 Literature Review

The first basic idea of Light Amplification by Stimulated Emission of Radiation or LASER came from an American scientist, Charles Hard Townes and two Soviet scientists, Alexander Mikhailovich Prokhorov and Nikolay Gennadiyevich Basov who shared the Nobel Prize in 1964. However, TH Maiman of the Hughes Research Laboratory at California, was the first scientist who experimentally demonstrated laser by flashing light through a ruby crystal in 1960. A few decades ago, it became possible to generate laser light pulses with a duration in the femtoseconds scale.

At present, a femtosecond laser is an excellent tool for producing laser pulses with very high intensity for laser-matter interactions, leading to various applications as well as laboratory experiments. It is widely used in thin film deposition (Womack et al., 2004), material characterization (Kabashin et al., 2003), drilling (Kamlage et al., 2003), micro or nano structuring (Costache et al., 2004), lithography, medical surgery (Shen et al., 2005) as well as fabrication of nanoparticles.

Many experiments have been done using femtosecond laser interacting with different materials at ambient environment (Amoruso et al., 2007), in gaseous as well as solid materials (Machmudah et al., 2011). Interaction of laser with solid materials is characterized by the ablation depth and width per pulse, as well as morphology on the target. The physical outcomes are determined by the way photon energy is transferred to the target.

Additionally, laser interaction with water has been explored (Barnes et al., 2016), with extensive reviews on underwater laser processing (Kruusing, 2004; Kruusing, 2004). It is important not only for fundamental research but also for applications such as synthesis of nanocrystals (Shen et al., 2004), (Yang, 2007) and medical applications especially when the laser is guided inside the human body to ablate tissues (Loesel et al., 1998).

Laser interaction with water enables us to understand the interaction between photons and fluids or soft matter with more complex assemblies. However, certain fundamental mechanisms in the interaction of intense laser with water have not been adequately explored. In picosecond laser ablation, there are many underlying mechanisms involved. First, during optical breakdown (Zysset et al., 1989) the electric field of the laser is sufficiently strong to rip apart the electrons from the atoms and molecules into ions and plasma through photoionization, photodissociation or photochemical processes. The focused region produces disruptive processes (Vogel et al., 1994) like nonequilibrium phase transition and/or explosive boiling. This is followed by cavitation of bubbles and shock waves (Juhasz et al., 1994) and photothermal process with thermal conduction at longer timescale. When the plasma is created (Noack & Vogel, 1999) the process escalates into breakdown dynamics (Schaffer et al., 2002). Cavitation is formed by spots of highly concentrated energy and ions that rapidly expands with hyper sonic velocity into bubbles as a result of the plasma and heat pressure accompanied by the generation of the pressure wave (Sakakura et al., 2007). A lot of work have been undertaken to study the dynamics and mechanism by looking at the shock waves generated in liquid (Brujan, 2008; Ohl et al., 1999; Peyre et al., 1996).

Further expansion of the plasma leads to the creation of cavitation bubbles (Akhatov et al., 2002), (Lim et al., 2010) and explosive boiling (Park et al., 1996). The kinetic behavior of nucleation and the growth of the bubbles have been studied by optical and acoustic means (Yavas et al., 1994). The mechanisms also involve thermodynamics and phase transition (Kim et al., 2001), particularly the change in temperature (Park et al., 1996) and pressure (Park et al., 1996; Brujan et al., 2008).

Subsequently, bubble expansion may decrease to subsonic velocity followed by implosion or collapse (Chen et al, 2004), (Lindau & Lauterborn, 2003) of the cavitation

bubble, creating secondary acoustic transients and light (Putterman & Weninger, 2000) accompanied by radially propagating acoustic waves (Yavas et al., 1994).

However, interactions of ultrashort laser pulses like femtosecond laser with water are more challenging scientifically due to the many physical mechanisms involved in the ultrashort time dynamics. During femtosecond laser focusing in liquid, nonlinear optical and photoionization processes dominate over the photothermal process. Examples of useful application are advanced materials processing (Sugioka & Cheng, 2014) and ultrafast sensing (Chiou et al., 2010). A few studies were involved in the interaction between femtosecond laser pulse and water from the energetic point of view (Sreeja et al., 2013) and in the aspect of spectroscopy (Ilyin & Golik, 2013) by measurements of emission spectra. Laser plasma interactions and supercontinuum generation produce white light (Chin & Lagacé, 1996). Thus, focused femtosecond laser in water is a very complicated process full of interesting physics. Figure 1.1 demonstrates the basic phenomena when femtosecond laser focused inside water including the outcome of this research work.

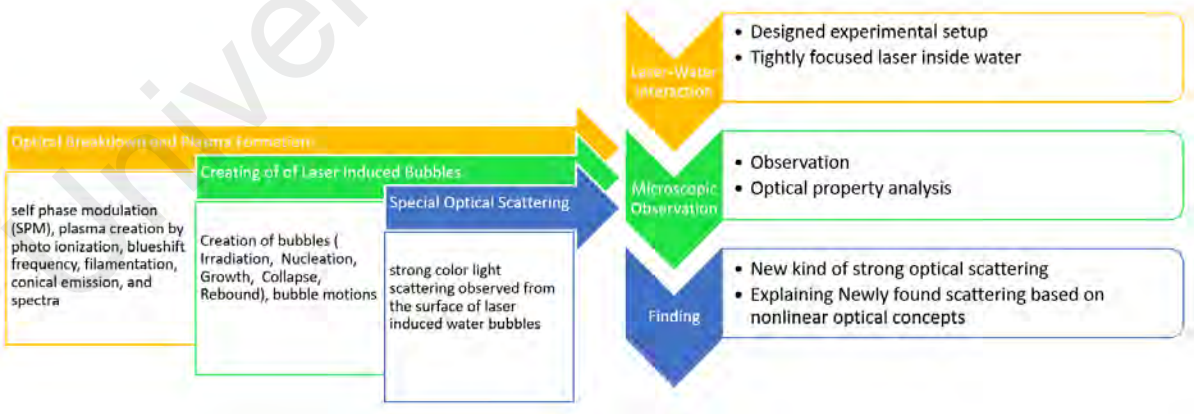

Figure 1.1: Phenomena and findings when high intense femtosecond laser focused inside water.

1.3 Objectives

The aim of this thesis is to describe the physical mechanisms of focused femtosecond laser pulses in water and explaining the experimental results based on fundamental concepts. Furthermore, as an additional objective, during the experimental study a new kind of optical effect by focused femtosecond laser pulses in water has been observed which is completely new and considered as a new challenge to study and explain our current understanding of fundamental concepts of nonlinear optics.

1.4 Outline

This thesis begins with the introduction in Chapter 1 which presents literature review corresponding to this research including research objective. Chapter 2 reviews the basic principle of lasers, femtosecond laser and pulse generation. Chapter 3 reviews the optical properties of matter, laser-matter interactions, and finally laser-liquid (water) interaction.

Chapter 4 describes the experimental procedure that had been developed for the work, including a short description of the equipment. The experimental result and related discussion are described in Chapter 5.

An overall conclusion and future directions for this research are provided in Chapter 6, forwarded by the appendices at the end of this thesis.

CHAPTER 2: CONCEPT OF LASER

It is important to discuss few fundamental concepts of lasers before discussing about laser-water interactions. After all, this experiment is a laser (particularly femtosecond laser) based experiment. So, a discussion of laser is necessary to be considered.

2.1 Laser Fundamentals

Light Amplification by the Stimulated Emission of Radiation or LASER is an artificial light generated by a device that produces intense beams of light which are monochromatic, coherent, directional, and highly non-divergent. The wavelength of laser light is extremely pure (monochromatic or single color) when compared to other sources of light, and all of the photons that make up the laser beam have a fixed phase relationship (coherence) with respect to one another. Laser light typically have very low divergence, they can travel over great distances and can also be focused into a very small spot with a very high energy density. Figure 2.1 expresses these properties of laser light.

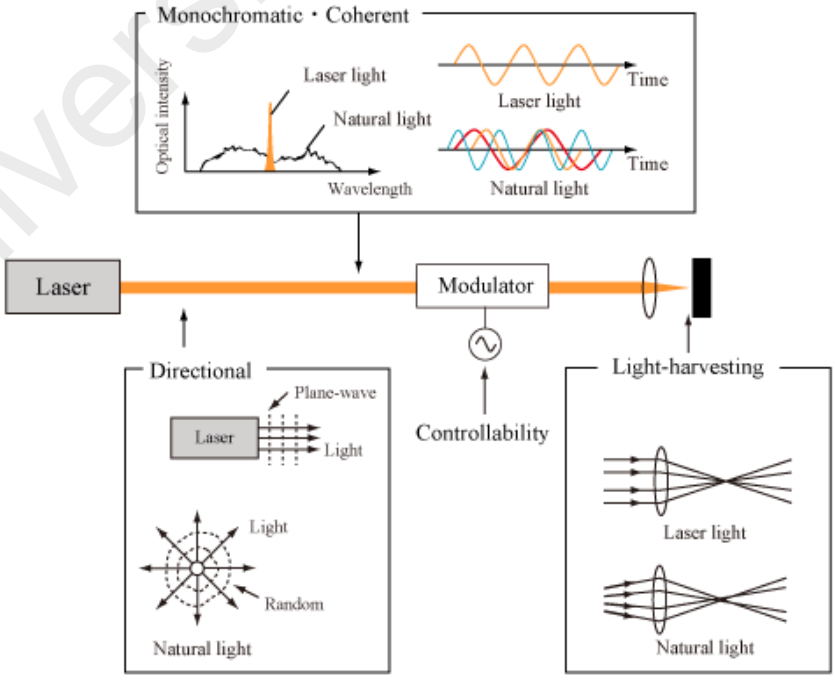

Figure 2.1: Laser and Characteristics of Lasers (Herd et al., 1997).

As mentioned, laser light is not found in nature so it is made artificially by a device which contains three components (Figure 2.2):

(i) Lasing material or gain or active medium usually solid (crystals, glasses and semiconductors); liquid (organic solvents and dyes; example: dye lasers); or gas. The type of laser is usually named after the lasing medium, and this is also the main factor determining the type of pump required and the wavelength of the resulting laser light.)

(ii) External energy source or pump (which may be an electric current or discharge, flash lamp, light from another laser, or a chemical reaction)

(iii) Optical resonator (this is laser's simplest form consists of two parallel mirrors: a highly reflective mirror and a partially reflective mirror, also called output coupler.)

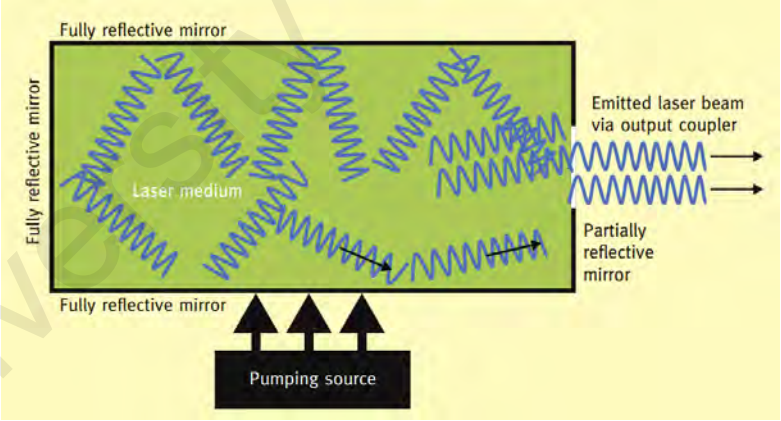

Figure 2.2: Laser Devices.

To explain internal mechanism of laser generation we need to take help of atomic theory, moreover, to avoid complexity we will describe using classical atomic theory which is sufficient to explain the principle of laser operation rather than modern atomic theory. According to classical theory atomic structure as a central nucleus composed of protons and neutrons surrounded by a cloud of electrons that orbit the nucleus in a series

of discrete orbitals. When energy is supplied to the atom, the electrons move from their low-energy orbitals near the nucleus to high-energy orbitals further away. The atom is said to absorb energy, and move from the ground state energy level (E_1) to an excited level (E_2). An electron in a high-energy orbital eventually returns to the low-energy orbital. As it does so, the difference in energy is released in the form of a photon, which has random phase and direction. This process is called spontaneous emission, and is the same process which causes an incandescent bulb, neon light, fluorescent tube, cathode ray tube or heating element to produce light.

The photon will have a frequency v and energy hv given by $E_2 - E_1 = hv$, where h is Planck's constant 6.63×10^{-24}J/s Hence, the wavelength of the light produced is determined by the amount of energy released when the electron returns to a lower orbital, and may be within the visible spectrum or beyond it (i.e. infrared or ultraviolet). If the photon collides with other excited electrons in the lasing medium, it will cause a second photon to be released which is identical to the original photon in its direction, phase, polarization and energy (wavelength). This is called stimulated emission. A cascade effect occurs as photons stimulate the emission of more photons, resulting in amplification or optical gain. The photons are initially released in random directions. However, as the chain reaction progresses, photons are reflected back and forth between the mirrors, and soon all atoms emit light along this axis. The output coupler is partially reflective, and allows a small number of photons to escape from the lasing medium. This is the usable laser light, which is directed to the target via a delivery system of fiber-optic light guides for visible light or a series of mirrors for infrared. For sustained laser action to occur, the majority of atoms must be maintained in the excited state (population inversion) by the continuous input of energy from the pump. If pumping is intermittent, a pulsed laser will result (Silfvast, 2004; Williams, 2008).

2.2 Device Types of Laser: CW and Pulse Laser and Some Quantities

There are two types of lasers based on their output laser light operation, either continuous wave (CW) or the pulsed laser. In a CW laser, a constant power is continuous output. In a pulsed laser, optical pulses are output with a constant repetition frequency. Figure 2.3 (a) shows a schematic of the CW operation and pulsed operation.

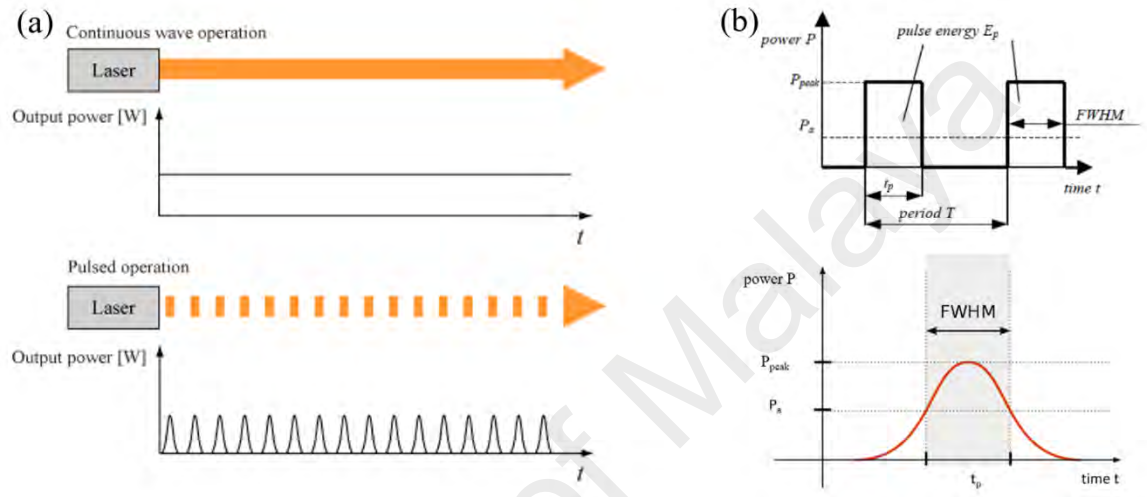

Figure 2.3: (a) CW Laser and Pulsed Laser & (b) Laser Quantity.

A laser is characterized by an average power P_a. A pulsed laser is generally characterized by a pulse duration T, repetition rate f_p, pulse energy E_p, and a peak power P_{peak}. These parameters of the pulsed laser are associated by the following expressions (also shown in Figure. 2.3 (b), FWHM is full wave half maximum). However, some of the quantities we do use frequently for measurements and practical applications.

repetition rate, $f_p = \frac{1}{T}$ (2.1)

peak power, $P_{peak} = \frac{P_a}{t_p f_p}$ (2.2)

intensity, $I = \frac{P_{peak}}{A} = \frac{E_p}{A t_p}$ (2.3)

fluence, $w = \frac{E_p}{A} = \frac{P_{peak} t_p}{A}$ (2.4)

pulse energy, $E_P = Pdt = P_{peak}t$ (2.5)

And, t_p = pulse width, P_a = average power, A = area

Table 2.1: Commercial Lasers.

Category	Pumping method		Laser	wavelength
Solid-state laser	current	compound semiconductor	laser diode	ultra violet~infrared
	flash lamp	flash-lamp pumping	Nd:YAG laser	1064 nm
			ruby laser	694 nm
			Nd: glass laser	1054 nm, 1062 nm
			Er: YAG laser	2.9 μm
			alexandrite laser	0.7 μm~0.82 μm
	laser	laser diode pumping	Nd:YAG laser	1064 nm
			Nd: YLF laser	1047 nm, 1053 nm
			Nd: glass laser	1054 nm, 1062 nm
			Nd: YVO_4 laser	1065 nm
			Yb: YAG laser	1030 nm
			Yb-doped fiber laser	1.0 μm
			Er-doped fiber laser	1550 nm
			Cr:LiSAF laser	0.65 μm~1.1 μm
			Er: YAG laser	2.94 μm
			Tm:YAG laser	1.8 μm~2.2 μm
		without laser diode pumping	far infrared laser	
			Ti:Sapphire laser	650 nm~1180 nm
			Ce:LiSAF laser	0.29 μm~0.30 μm
			Cr:Forsterite laser	1.13 μm~1.37 μm
			Ho:YLF laser	0.75 μm~2.06 μm
			Ho:YAG laser	2.09 μm~2.10 μm
Liquid laser			dye laser	300 nm~1200 nm
Gas laser	discharge	metal laser	copper vapor laser	511 nm, 578 nm
			He-Cd laser	325 nm, 442 nm
		non-metal laser	He-Ne laser	633 nm
			Ar ion laser	275 nm~1090 nm (many oscillation lines)
			Kr ion laser	337 nm~858 nm (many oscillation lines)
			N_2 laser	337 nm
			CO laser	5~7 μm
			CO_2 laser	9~11 μm
	electron beam	excimer laser	KrF laser	126 nm~351 nm
			XeCl laser	
			ArF laser	
			F_2 laser	
Chemical laser	chemical reaction		HF laser	2.7 μm~2.9 μm
			iodine laser	1.3 μm

It is important to note that beside CW and Pulse, lasers are also categorized into solid-state laser, liquid laser, gas laser, and chemical lasers. The categories and commercially available lasers are mentioned in Table 2.1 (Hitz, Ewing & Hecht, 2012).

2.3 The Femtosecond Laser and Pulse Generation

Nowadays almost all the research laboratories, dealing with high-resolution spectroscopy and non-stationary processes, use femtosecond lasers. Ti: Sapphire laser is the most popular among them. Femtosecond laser pulses are related to laser pulses with a duration on the femtosecond time scale. 1 fs or femtosecond = 1×10^{-15}second. The short optical pulse allows for visualization of ultrafast dynamical process such as fluorescence and excited state absorption, and the high peak power of the pulse allows application in nonlinear spectroscopy, material processing in such process as multi photon absorption, optical harmonics generation, materials ablation, etc. Time-resolved spectroscopy, multiphoton imaging, micromachining, communications, isotope separation, and generation of intense bursts of x-rays are among the large number of applications of femtosecond laser pulses (Kaiser & Auston, 1993).

The pulse energy comes out directly from a femtosecond laser is in the range of nanojoules. These femtosecond laser pulses then amplified to the microjoule and millijoule level to become fully potential. However, it does not have direct amplifying option since the high pulse intensity is the causes of damaging of the optics in the amplifier. The reason behind is the non-linear effects induced by the very high intensity of the femtosecond laser pulses. So, a technique called Chirped pulse amplification (CPA) is used for generation of ultrashort laser pulses without damage of the active medium or optics used. The concept of CPA is interesting, a femtosecond pulse train produced by the oscillator (Ti:Sapphire) is stretched in a pulse stretcher to reduce the intensity. The stretched pulse is then amplified to increase its energy. Finally, the amplified stretched

pulse is compressed to produce energetic femtosecond laser pulses as shown in Figure 2.4 (Liu et al., 1997).

More about CPA: To generate a laser pulse within a femtosecond time domain, the active medium should have a broad emission bandwidth. Because of the relationship between the pulse duration and its spectral bandwidth is associated by the Fourier-transform-limited pulse relation: $\Delta v \Delta t \geq K$, where Δv frequency bandwidth measured at full-width at half-maximum (FWHM), Δt is the FWHM in time of the pulse and K is a constant depending only on the pulse shape, for an example, it equals 0.441 for Gaussian. The requirement of sufficient bandwidth during the amplification process limits the number of materials (active media) that can be used for the generation and amplification of femtosecond laser pulses to three types of materials: dye lasers (580-900 nm), Excimer lasers (ultraviolet), and solid state media (Patterson et al., 1990).

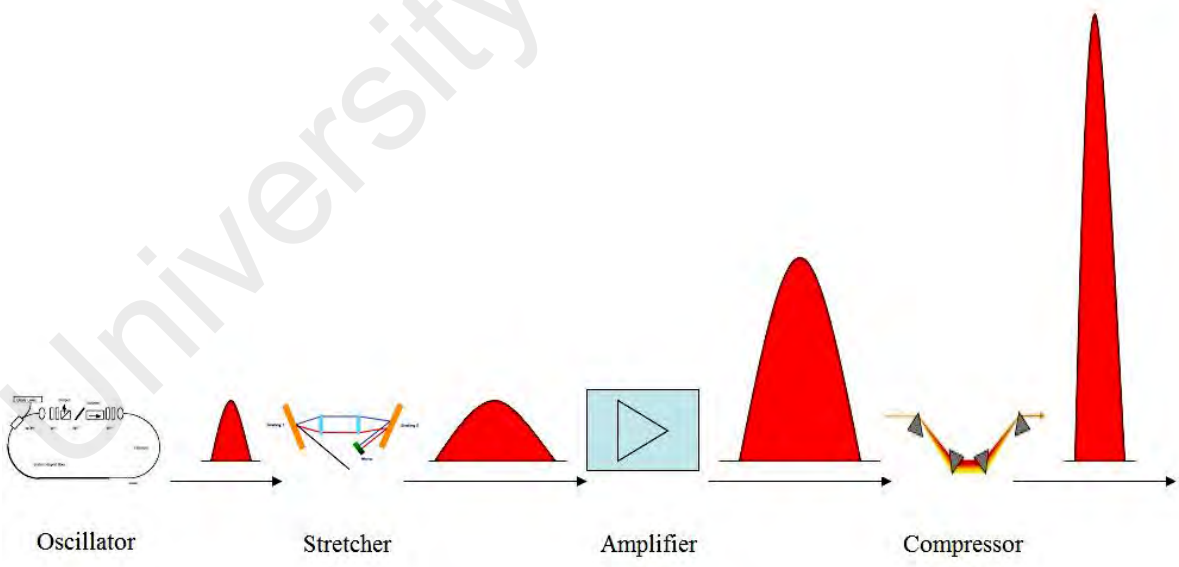

Figure 2.4: Chirped Pulse Amplifier (CPA).

Based on CPA, a femtosecond laser system consists of four sections:

a) The oscillator, which generates the femtosecond laser pulses:

Titanium-sapphire (Ti:Al_2O_3) crystal, the gain medium of the laser oscillator, is commonly used for femtosecond pulse generation in the near infrared. Its broad gain bandwidth (~ 200 nm) and its high thermal conductivity and high damage threshold make it suitable for the generation and amplification of ultra-short laser pulses of a few femtosecond pulse width at the 800 nm central wavelength (Sullivan et al., 1991). The minimum pulse duration that is obtained from a spectrum with wavelength difference $\Delta\lambda$ nm at FWHM can be calculated from Fourier transformation: $\Delta t = k\frac{\lambda_0}{\Delta\lambda c}$, where λ_0 is the central wavelength and c is the velocity of light. This yields an expected minimum pulse duration for Ti:Sapphire of about 5 fs. Ultra-short laser pulses are generated by mode locking, this is a technique by which a laser can be made to produce laser pulses of extremely short duration, on the order of picoseconds (10^{-12}s) or femtoseconds (10^{-15}s)). This mode-locked laser typically generates light pulses at high repetition rate (~108Hz). It is mentionable, CW laser and pulse laser are also pumped by CW. The difference is mode-lock.

When light propagates through a dispersive medium, different frequency component travel at different speeds (group velocity dispersion) because of the dependence of the refractive index of the medium on the wavelength. These result in stretching out a short pulse made of different frequency components. In case of positive dispersion (propagation of a pulse in media with normal dispersion), higher frequency components travel slower than lower frequency components and the pulse is said to be positively chirped. The opposite situation, when the pulse travels through a medium of negative dispersion, higher frequency components travel faster than lower frequency components and the pulse is said to be negatively chirped. In an ultra-short laser oscillator, positive

dispersion in the gain medium and other optical components must be compensated. This can be done by inserting optical components with negative dispersion (pair of prisms or specially made chirped mirrors) in the oscillator as shown in Figure 2.5 where Ti:Sapphire oscillator which consists of two double chirped mirrors (DCM1, DCM2) and fused silica (FS) prism pair for compensation of dispersion (Sutter, et. al., 1998).

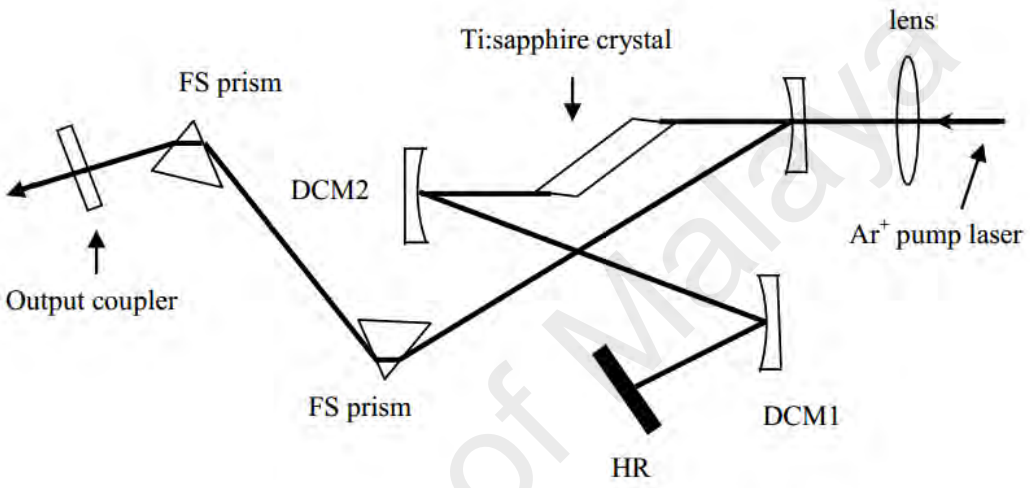

Figure 2.5: Ti: Sapphire oscillator (Sutter et al., 1998).

b) The stretcher, which consists of a pair of optical gratings used to expand the femtosecond pulse width:

The laser pulses obtained from the Ti: Sapphire oscillator have energies of the order of a nanojoule and pulse duration of a few femtoseconds. For amplification of these pulses without damage of the optics used, the pulses are first stretched and then amplified. The pulses are stretched in time using the dispersion properties of a pair of gratings arranged to give positive group velocity dispersion. Figure 2.6 is showing the arrangement of a grating-pair pulse stretcher where G1 and G2 are diffraction gratings, L1 and L2 identical lenses separated by twice their focal length *f*. M is a mirror acting to double pass the beam through the system. The amount of pulse stretching is determined from the distance:

$Ls = 4f - L_{sg}$ where L_{sg} is the stretcher grating separation and f is the focal length (Backus et al., 1997).

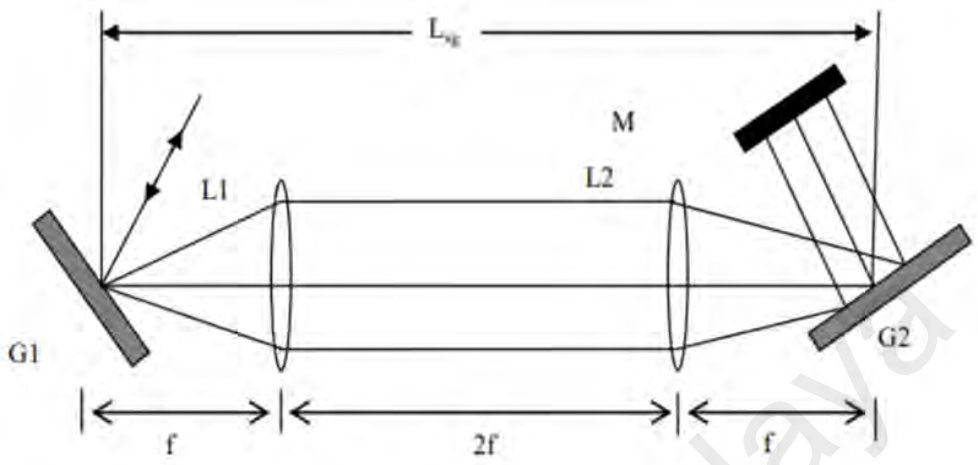

Figure 2.6: A schematic diagram of a stretcher (Backus et al., 1998).

c) The amplifier, which is used to amplify the stretched signal:

After being stretched in the optical stretcher the oscillator generated femotosecond laser pulse generates and safely amplified without exceeding the damage threshold of the amplifier materials. Regenerative and multipass amplifiers are most widely used for the amplification of femtosecond laser pulses. Regenerative amplification is a well-established technique for efficient generation of microjoule and millijoule energy ultra-short pulses from solid state lasers (Lenzner et al., 1995). In regenerative amplifiers (Figure 2.7 (a)) the low energy stretched pulse is injected and trapped in a laser cavity similar to that of the oscillator using a fast-switching Pockels cell and thin film polarizer (Cheriaux, G., & Chambaret, J. P. 2001). For further amplification of the laser pulses, a multipass amplifier is used (Figure 2.7 (b)). In the multipass amplifier the laser beam passes through the gain medium multiple times without being trapped in a cavity.

a) Regenerative amplifier

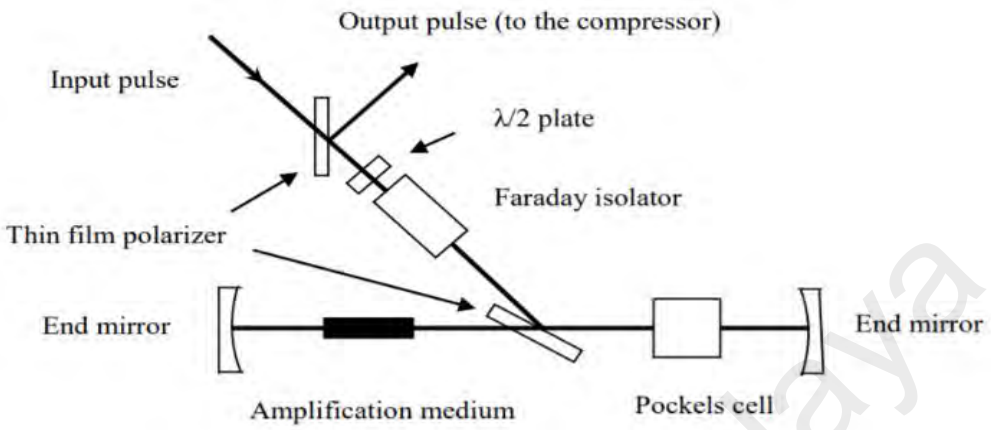

b) Multipass amplifier

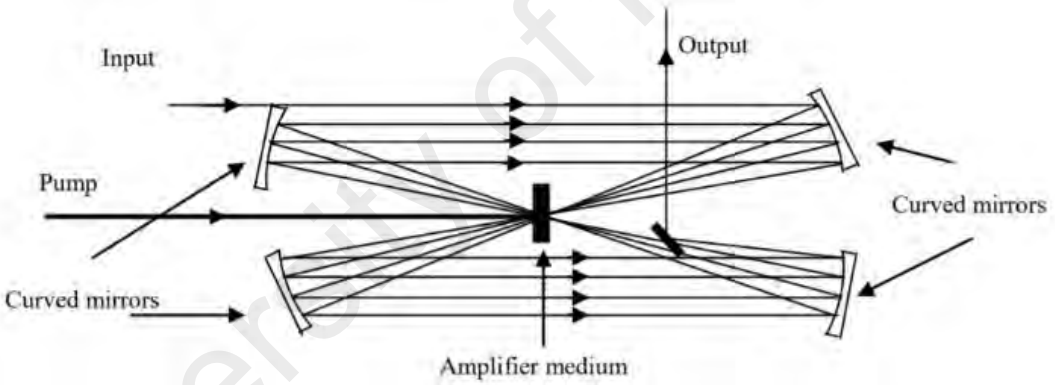

Figure 2.7: Two schematic diagram of amplifiers (a) Regenerative amplifier & (b) Multipass amplifier (Cheriaux, & Chambaret, 2001).

d) The compressor, which is used to compress the amplified pulses

Compression of amplified chirped pulses is the last stage in the generation of femtosecond laser pulses. This step is accomplished by using a grating pair similar to that used in the stretcher but arranged in such a way to give opposite dispersion, as shown in Figure 2.8.

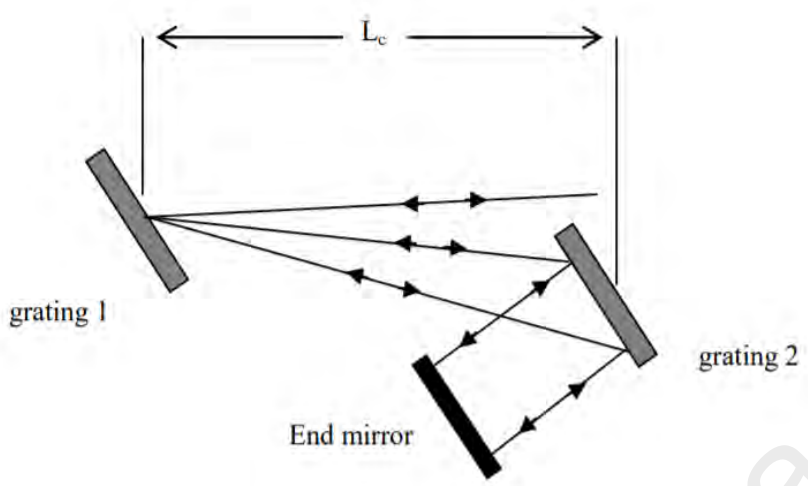

Figure 2.8: Schematic diagram for pulse compressor (Backuset el al., 1998).

The amount of pulse compression is determined by the grating separation L_c and the shortest pulses can be obtained when the stretcher grating separation L_{sg} equals the grating separation of the compressor. By changing the compressor grating distance L_c, continuous pulse widths can be obtained from the shortest compressed pulse to the uncompressed stretched value (Backus et al., 1998).

CHAPTER 3: REVIEW ON LASER WATER INTERACTION

The focused ultra-short laser into the water shows a sequence of separate events, where related but many different underlying mechanisms are involved, which is significantly different from laser and other material interaction.

At the beginning, a focused ultra-short pulsed laser creates plasma on the medium, similarly when the pulse ultra-pulse laser is focused into water it creates plasma, and the phenomenon of laser induced plasmas in water can be described by a sequence of events: creation of plasma and optical breakdown, filamentation, optical cavitation bubbles creating and evaluation, shockwave, and white light super continuum emission (Felix et al., 1997).

The detailed calculation of plasma formation and related events in aqueous media is difficult; primarily because liquid water is a surprisingly complex medium, whose structure and physical properties are still not completely understood despite decades of study (Grand et al., 1991).

Therefore, this work has been done experimentally, although some theoretical modeling has also been done, typically to aid in evaluating experimental data.

3.1 Creation of Plasma, Optical Breakdown and Filamentation

In the focus region the high intense electric field of the pulse laser is strong enough to rip apart the electrons from atoms and molecules into ions and create plasma through photoionization or optical breakdown and photo chemical process (Zysset et al., 1989).

This breakdown occurs in two ways, direct ionization of the medium by multiphoton absorption and cascade ionization, also known as avalanche ionization. These multiphoton and cascade breakdowns can occur in solids, liquids, or gases. In multiphoton

ionization, two or more photons are absorbed simultaneously by the medium particle so that there is enough energy to ionize it. High irradiances are usually required for occurring ionization where multiple photons are involved. This process is known to create 'seed' electrons in pure medium. However, this is for solids and liquids; the seed or free electrons do not truly exist in the same sense in gas plasmas. In condensed medium we have both electrons which are bound to a particular molecule or lattice site and electrons which are 'quasi-free', i.e. their kinetic energy is high enough that they can move through the liquid or solid lattice without being trapped by localized potential wells. When the medium breaks down, transitions between bound and quasi-free states both are the equivalent to molecular ionization in gases.

In order to obtain an analytic expression for the threshold irradiance corresponding to multiphoton breakdown in aqueous media, a modified version of Keldysh formula for multiphoton ionization in semiconductors was employed (Kennedy, 1995).

So, if W is multiphoton ionization probability, I_0 is the peak optical irradiance then we find a set of equations,

$$W = A[BI_0]^x \tag{3.1}$$

$$A = \left(\frac{2}{9\pi}\right)\omega\left(\frac{m\omega}{h}\right)^{\frac{3}{2}}\exp[2k]\phi(z)\left(\frac{1}{16}\right)^k \tag{3.2}$$

$$B = \left[\frac{e^2}{m}E_{ion}\omega^2 c\varepsilon_0 n_0\right] \tag{3.3}$$

$$z = \left[2k - \frac{2E_{ion}}{h\omega}\right]^{\frac{1}{2}} \tag{3.4}$$

Where k represents the number of photons of energy $h\omega$ needed to ionize, E_{ion} is the transition energy across the band gap (ionization energy), m represents the exciton reduced mass, $€$ is the electron charge, c is the vacuum speed of light, ε_0 is the permittivity of free space, n_0 is the index of refraction of the medium at frequency ω, and the function

$\varphi(z)$ represents Dawson's Integral (Kennedy, 1995). The probability W gives the number of ionizations (or free carriers generated) per unit volume per unit time.

Breakdown by cascade ionization occurs in two steps: (i) cascade initiation through the creation of seed electrons and (ii) cascade build up to high free electron densities. Cascade initiation requires one or more free electrons to be present in the focal volume at the beginning of the pulse. In an impure medium, these 'seed' electrons are most likely to come from ionization of impurities by thermal excitation, which produces an initial free electron density in the focal volume prior to the pulse. In a pure medium, seed electrons must be produced by ionization of a few molecules in the medium through multiphoton absorption (Kennedy, 1997).

To study cascade ionization, two models are used; lucky electron model, which is used for solid and the rate equation model, which is used in gas, solid and aqueous media (DeMichelis, 1995).

A generic rate equation for cascade formation has the form,

$$\frac{\partial \rho}{\partial t} = n\rho - g\rho - v_A\rho - v_R\rho^2 \qquad (3.5)$$

The first term on the right-hand side represents the increase in free electron density, ρ due to cascade ionization, where the cascade ionization rate, n is the probability per unit time that a free electron will have an ionizing collision with a bound electron. In the most general formulation, the net cascade ionization rate combines the effects of free electron energy gain by inverse bremsstrahlung absorption and free electron energy loss in nonionizing collisions with heavy particles. The last three terms represent losses of free electrons due to: (i) diffusion out of the focal volume, where g is the diffusion rate, (ii) attachment of neutral molecules (or trapping in localized potential wells), where v_A is the rate of attachment (or trapping), and (iii) electron-ion (or electron-hole) recombination,

where v_R is the rate of recombination. A term representing multiphoton ionization can also be added to allow for multiphoton initiation of cascade breakdown or for the transition from cascade to multiphoton ionization as the dominant breakdown mechanism in the femtosecond pulse width regime (Bloembergen, 1974).

A laser pulse focused into a volume of water or aqueous fluid will cause breakdown when the irradiance in the focal volume surpasses the breakdown threshold. The dense plasma formed by the breakdown is heated by inverse bremsstrahlung absorption while the laser pulse remains in the focal volume. Plasma temperatures of 6000-15,000° K (Barnes & Rieckhoff, 1968; Doukas et al., 1991) and plasma pressures as high as 20-60 kbar (Vogel et al., 1994) have been measured for the breakdown in aqueous media. Bremsstrahlung emission from free electrons and emission from electron-ion recombination combine to produce a visible 'flash'; i.e. a broadband plasma emission from the ultraviolet to the infrared. This flash is commonly used as an experimental indicator of laser induced breakdown spectroscopy (Vogel et al., 1999; Zysset et al., 1989). The high temperatures and pressures can lead to plasma expansion at supersonic velocities and the creation of a shock wave.

The moving breakdown model for plasma growth (Docchio et al., 1988; Hammer et al., 1997) use of the Planck blackbody equation to calculate plasma temperatures from emission spectra.

Next the passage of the pulse the plasma continues to expand and vaporize the liquid, creating a cavitation bubble of water vapor, which grows about the breakdown site. When cooling and plasma decay reduces the interior pressure, the cavitation bubble collapses. If enough energy is stored in the bubble, the collapse may release a second shock wave and heat the gas sufficiently to cause the bubble to re expand (Hickling & Plesset, 1964).

After that, while high intense laser focused inside water that moment under comparatively loose geometrical focusing condition (because of water) femtosecond laser pulse can form electron plasma strings that extend far beyond the focal spot, have a constant diameter, and their intensity is to a large extent not affected by fluctuations of the laser pulse energy. This is called femtosecond filamentation inside water (Hao et al., 2011). Also, can be said, when femtosecond laser focused inside the water then dynamic balance between the optical Kerr self-focusing effect and the defocusing effect is caused by the plasma which produces laser filamentation inside the water (Liu et al., 2003).

The Kerr effect is represented by a nonlinear term in the index of refraction which is proportional to the optical irradiance *n* (Soileau et al., 1989),

$$n = n_0 + n_2 I \tag{3.6}$$

At high irradiances, and in materials with a significant nonlinear index n_2, nonlinear self-focusing can produce beam narrowing or even catastrophic beam collapse (filamentation) leading to breakdown. Self-focusing is both an irradiance dependent and a power-dependent process. The critical power for self-focusing (Marburger, 1975) is the input power for which a laser beam with vacuum wavelength λ, will undergo catastrophic self-focusing when propagating a long distance through a medium whose linear and nonlinear indices at the vacuum wavelength are given by n_0 and n_2.

$$P_{cr} = \frac{0.15(\lambda)^2}{n_0 n_2} \tag{3.7}$$

The filamentation under water also shows some interesting phenomena, such as a) white light continuum generation, b) conical emission and c) bubble generation by optical cavitation (Mizushima & Saito, 2015).

3.2 Optical Cavitation Bubbles

Plasma inside water vaporizes liquids and creates optical cavitation bubbles around the breakdown site. When cooling and plasma decay reduces the interior pressure, the cavitation bubble collapses. If enough energy is stored in the bubble, the collapse may release a second shock wave and heat the gas sufficiently to cause the bubble to re expand. And, for high energy breakdown events, multiple expansions and collapses may take place, ending only when the stored energy is insufficient to sustain bubble growth (Vogelet al., 1996) (Vogel et al., 1989). The movements of the generated bubbles in water are mainly driven by the filament-induced shock waves, Coulomb force and the pressure force induced by water density gradient (Sakakura et al., 2001).

Thes, from the discussion so far we can say, the life of an optical cavitation bubble can be further investigated in five stages:

i) Irradiation; it's the period for which absorption of optical energy occurs, for a CW laser, this period occurs throughout the cavitation process with a decrease in irradiation as the bubble grows in diameter. For a pulsed laser, irradiation occurs only when the laser is active. Previous studies have shown that irradiation with a pulsed laser excites the liquid so intensely that the atomic level is affected. The liquid molecules release electrons and form a plasma which continues to super heat the surrounding liquid even after, a process that CW lasers cannot produce.

ii) Nucleation; it is the breaking down of the liquid's molecules which allow for energy to lead to vaporization.

iii) Growth; the is when bubble begins to grow and sees sizes of microns for pulsed lasers and diameters up to 5 mm for CW lasers. Higher laser power

correlates to smaller and faster formation of bubbles (Rastopov & Sukhodol'sky, 1990).

iv) Collapse; the bubbles collapse as soon as the pressure within the bubble falls short of the local pressure outside, and

v) Rebound; after collapsing it also shows periodic rebounding and collapse for a very short time. This is also the reason of the formation of powerful acoustic waves and secondary waves of bubbles (Csuka et al., 2016).

It is necessary to mention each period or stage of the bubble develops differently for CW and pulsed lasers (Sakakura et al., 2007), where for CW laser, the mechanism is thermal process and for pulsed laser (i.e. femtosecond laser), the nonlinear optical and photoionization process dominate over photo thermal process (Sugioka & Cheng, 2014). Therefore, optical cavitation can be classified into two types: one, thermocavitation, where CW laser does use and this bubbles are created by heated up and two, ionocavitation, where pulsed laser creates bubbles are generated by ionizing liquid into plasma. More details have been added to **Appendix A** to discuss mathematical formalization of bubbles and **Appendix B** to discuss motions of bubbles.

3.3 White Light Continuum Generation and Conical Emission

A focused laser beam in medium results in the emission of light with a broad frequency range known as supercontinuum emission (SCE), extending, typically, from the ultraviolet to near-infrared spectral range. It is associated with filamentation of femtosecond laser pulses occurs when the laser power exceeds critical power for the self-focusing in the medium (Kiran et al., 2010).

To simplify the explanation, we assume that the self-focused wave is a plane wave. In this plane wave approximation, the plane wave front at the self-focus is given by the function, $F(z,t)$.

$$F(z,t) = \exp\{i[\omega_0 t - kz]\} = exp\left\{i\left[\omega_0 t - \frac{\omega_0 n}{c} z\right]\right\} \quad (3.8)$$

$$n = n_0 + \Delta n(t) \quad (3.9)$$

$$\Delta n = n_2 I(t) - \frac{4\pi e^2 N_e(t)}{2m_e \omega_0^2} \quad (3.10)$$

where z is the propagation distance, ω_0 is the central angular frequency of the laser. $n_2 I(t)$ is the Kerr nonlinear refractive index of the neutral gas (fluid), $I(t)$ is intensity. $N_e(t)$ is the electron density generated through tunnel ionization of the molecules and e and m_e are the charge and mass of an electron. The electron-ion recombination time is normally of the order of many nanoseconds, much longer than the femtosecond time scale of the pulse. Hence, the generated plasma could be considered as static during the interaction with the pulse (Chin, 2010).

Experimentally observed spectra for aqueous laser induced breakdown have been found to exhibit a blackbody spectrum. The Planck blackbody distribution can therefore be used to calculate estimated plasma temperatures from the emitted irradiance spectra. (Barnes, & Rieckhoff, 1968)

$$I(\lambda, T) = I_0 C_1 \lambda^{-5} \left[exp\left(\frac{hc}{\lambda k_B T}\right)^{-1}\right] \quad (3.11)$$

Here T is the plasma temperature in degrees Kelvin, h is Planck's constant, and k_B is Boltzmann's constant. The parameter C_1 is a product of several physical constants which appear in the derivation of this equation and has the value 14388 μm³. The blackbody distribution peaks at a wavelength λ which is inversely proportional to the temperature; thus, a peak at a shorter wavelength indicates a higher temperature. Temperatures obtained from this equation are necessarily estimates since the true plasma temperature will vary in both space and time. The surface temperature will not only be cooler than the

plasma interior but will also make a larger contribution to the measured spectrum, since radiation emitted from the plasma will be partially reabsorbed before reaching the surface (Hecht, 1987).

Other than supercontinuum emission, conical emission is a manifestation of self-phase modulation in the radial direction. Conical emission is the cause of colorful rings, those are rainbow-type colored rings, generated around the central white spot. They are produced by blue shifted radiation diverging into rings. As a note it is needed to be mentioned in gaseous medium rings are visible but in aqueous medium conical emission does split into colors rather than rings. More details on this topic can be found in work of Kosareva (Kosareva et al., 1997).

CHAPTER 4: EXPERIMENTAL PROCEDURE

This chapter discusses the setup of the experimental setup and procedures, which can be separated into two main parts: (1) experimental setup model, (2) description of the equipment description for detection and data collection.

An explanation of results and captured images based on the calibration of the spectrometer and microscopic observations are also provided in this chapter.

4.1 Experimental Setup Model

In this work, a commercial Ti: Sapphire femtosecond laser amplifier system (Coherent Inc.) is employed that generates laser pulses with duration of 50 fs, energy of 2.5 mJ per pulse with a central wavelength of 800 nm and repetition rate 1kHz, giving an average power of 3.5 W with an output of the peak powers of 5×10^{10} W, The laser beam, with diameter 1 cm, is focused into the water by a biconvex objective lens (2.5 cm focal length) from the side of the water container. The water specification will be found in **Appendix C**. The corresponding numerical aperture is : $n \sin(\tan^{-1}(0.5/2.5)) = 0.26$ for $n = 4/3$ in water. At an estimated focused diameter of 70 μm, the peak intensity is about 2×10^{14} W/cm^2, which is in the tunnel ionization regime where plasma formation balances the Kerr nonlinearity that creates self-phase modulation, giving rise to filamentations.

A schematic of the experimental setup for the laser-water interaction is shown in Figure 4.1. The curvature of the container causes some refraction that slightly enhances the focusing effect of the lens, but it does not significantly affect the results obtained. During the interaction, a CCD camera (Thorlabs) was placed in front of a neutral density filter to record images and live videos of the laser-water interactions. Another camera was placed on top of the eyepiece of the microscope to record at the microscopic level. In addition to imaging, a spectrometer (Ocean Optics) was placed on another side of the

setup. Light emitted and scattered from the focused region of the water can penetrate the transparent container and its spectrum detected by a spectrometer (Ocean Optics) without a fiber or a collimating lens. The spectrum was collected at the center of the supercontinuum light cone and along the transverse direction.

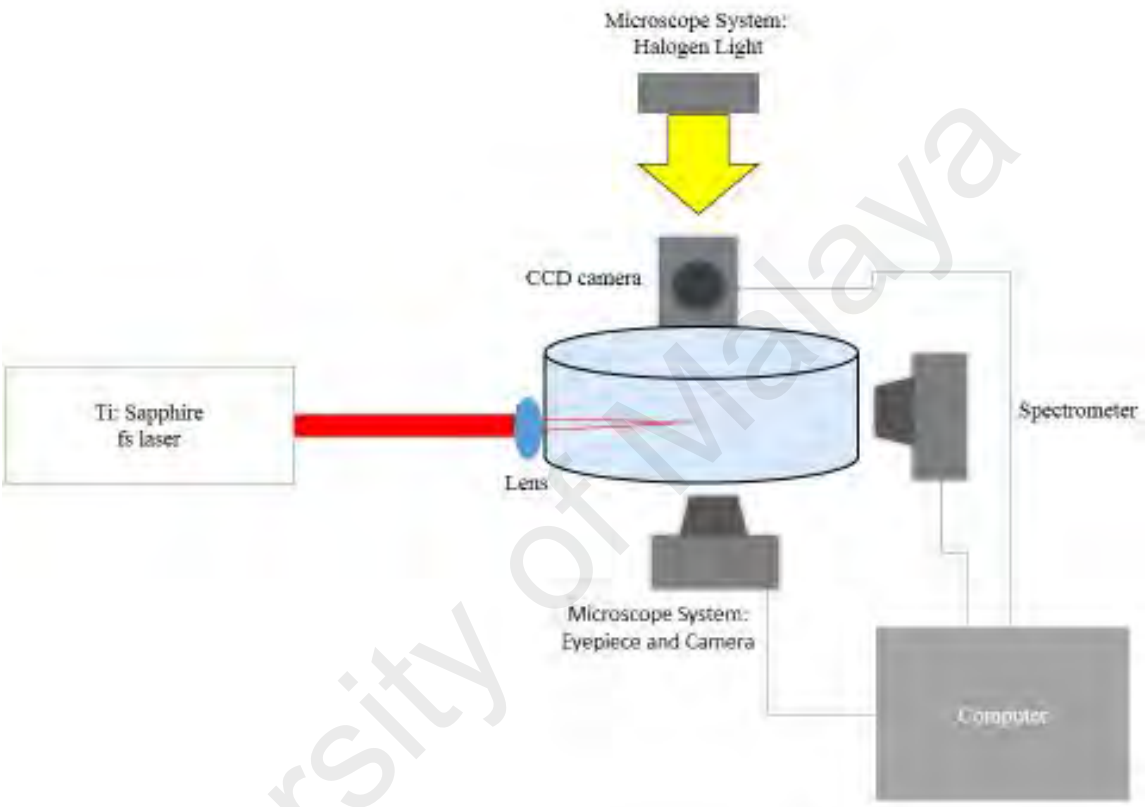

Figure 4.1: Schematic Diagram of Experimental Setup.

We chose this particular setup (Figure 4.1) on account of the fact that make sure less mechanical lose of laser energy before concentrating inside water by focusing using our experimental lens. Spectrometer and CCD cameras are soft hand movable to configure without any changing of the position of the experimental object. Despite the fact that there is a limitation of this setup, microscope system is not movable because the lens of microscope is static in microscope system which doesn't allow smooth observation.

4.2 Equipment Description and their uses

The Libra system employed in this work is a one-box, computer-controlled, kHz-repetition-rate, Ti: Sapphire laser. Libra also allows for a wide choice of pulse energy, pulse duration, and repetition-rates. The Libra offers >1-4 mJ at 1 kHz, it is also commercially available in 1 kHz, 5 kHz and 10 kHz configurations with pulse durations smaller than 50 fs or smaller than100 fs.

The output power of the system is calibrated by changing the input current as show in in Figure 4.2.

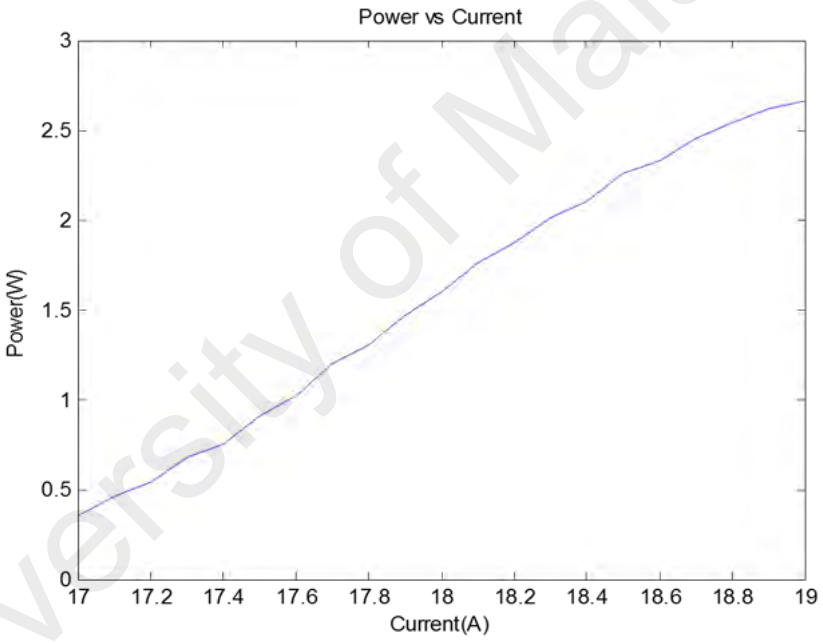

Figure 4.2: Current VS Power Curve.

To observe the water-laser interaction, a microscope system called Olympus Ix73, which is well known for its simplicity and exceptional flexibility is employed the experimental object in place on the microscope's platform and used view finder to watch the output live.

However, the system is not suitable for our required imaging without any modification as it is too much light sensitive that the camera was unable to handle. So, a much higher degree of brightness sensitive camera was placed on eye finder and using that the required images and live video shots were captured and recorder.

The spectrometer is employed for spectroscopic analysis. It is a small-footprint, high-resolution spectrometer that is well suited for applications such as wavelength characterization of lasers and LEDs, monitoring of gases and monochromatic light sources, and determination of elemental atomic emission lines. However, the input hole is very small and it is too sensitive that to get exact value using spectrometer was so difficult, to solve this problem the spectrometer were placed on a 3-axis stage to allow 3 dimensional control and obtain consistent results.

The water was contained in a transparent plastic Petri disk. Multiple numbers of Petri disks were used to get correct imaging, as for tiny displacement between lens and Petri disk's placement became the reason of Petri disk's surface burning. The distance between petri disk and lens were adjusted minimum to make sure there are no energy lose when focused laser beam was traveling from lens to petri disk surface before entering inside water.

Finally, the cameras employed in this work were a commercial Canon, and Thorlab CCD camera and a Nikon digital single lens reflection camera. Before using the CCD camera a neutral density filter was placed in between camera and light source, without that CCD camera was not functioning for its high light sensitivity. The canon camera was placed on our microscope system's eyepiece such a way that it can record macro level images and capture videos through the eyepiece.

CHAPTER 5: INVESTIGATED RESULT AND DISCUSSION

To describe this femtosecond laser-water interaction experiment it is necessary to mention few selected observations, provide explanation of observations and discuss some mechanisms based on available theories. All these can be classified as:

1. Laser induced breakdown in water and filamentation
2. Colors and blue shift by plasma and white light spectra
3. Creation of Bubbles
4. Rapid Generation of Bubbles
5. Colored light scattering by bubbles
6. Approximate position and size distribution of scattering color bubbles
7. Laser power and Related Effects on multi Spectral Colors
8. The forces on bubbles

As discussed in chapter 3, during the laser-water interaction and tightly focused laser beam few extreme physical phenomena become visible, they occur spontaneously, and, can be mentioned as, generation of white light by water, explosive boiling of water and vaporization, plasma and production of hydrogen, oxygen and peroxides, shock wave formation and propagation, bubble formation, their growth, collapse and re-expanding as like oscillation. These phenomena are well known (as discussed in Chapter 3) and we have observed them in our experiment too. But all are not related to our experimental aim, so many of them are not discussed in this study

The study has been done in microscopic level by a microscope system, the microscope system has halogen light so some of our observation has done under halogen light some of them without halogen light based on necessity (Figure 4.1), which leads us to observe

laser induced bubbles, their activities, explosive boiling, and surrounding environment more clearly at no-laser focused region. The captured images and recorded video clips under halogen light and without halogen light are demonstrated below.

Under the microscope, illuminated by a halogen light from above, it is observed the formation of bubbles and twinkling or sparkling of tiny bright points of lights with various colors, namely blue, purple, green, orange, and red, near the focused region under the water (Figure 5.2) is observed. Interestingly, yellow light was observed, which corresponds to the dip at 600 nm in the spectrum of (Figure 5.4). It is observed that, the bubbles are approximately 20 microns in diameter and they appear dark under the microscope light illumination (Figure 5.3), with a bright center, due to the regular lensing/focusing effect of the translucent sphere (Sankin et al., 2005).

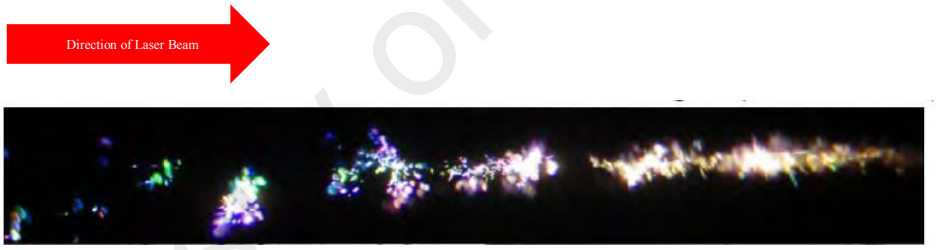

Figure 5.1: Twinkling color lights without halogen light.

Figure 5.2: Twinkling color lights with halogen light.

5.1 Laser Induced Breakdown in Water and Filamentation

An intense laser pulse was focused into a volume of water will cause breakdown when the irradiance in the focal volume surpasses the breakdown threshold. The dense plasma formed by breakdown was heated by inverse bremsstrahlung absorption while the laser pulse remained in the focal volume. This kind of plasma's temperature was recorded 6000-15,000 °K (Barnes & Rieckhoff, 1968) and plasma pressure as high as 20-60 kbar (Doukas et al., 1991). The high temperatures and pressures led to plasma expansion at supersonic velocities and the creation of a shock wave. Then, through the passage of the pulse, the plasma continued to expand and vaporize liquid, before creating cavitation bubbles of water vapor, which grow about the breakdown site. After that, inside water, for comparatively loose geometrical focusing condition (because of dynamic balance between the optical Kerr self-focusing effect and defocusing effect in water) femtosecond laser pulse formed electron plasma strings that extend beyond the focal spot, these strings are called femtosecond filamentation inside water (Figure 5.3). Due to laser filamentation inside water; white light continuum generation, conical emission and bubble generation by optical cavitation become visible.

Figure 5.3: Laser induced breakdown in water and filamentation.

5.2 Colors and Blue Shift by Plasma and White Light Spectra

The spectrum of the white light scattered in the forward direction contains predominantly blue-shifted frequencies with respect to the input pulse. The blue shifting is due to self-phase modulation (SPM) of plasma resulting from tunnel ionization of the water molecules by focused laser pulse that causes a rapid increase in the electron density, which in turns causes divergence/defocusing of the intense laser field. It is also enhanced by self-steeping (Aközbek et al., 2001)

$$\Delta\omega = \frac{d\Delta\varphi}{dt} = \frac{d}{dt}\left(-\frac{\omega}{c}L\Delta n\right) \tag{5.1}$$

This is frequency shift $(\Delta\omega)$ which is related to the change in the reflective index (Δn), here, (ω) is the laser frequency and *(L)* is the interaction length.

$$\Delta n = \sqrt{\varepsilon + \Delta\varepsilon} - \sqrt{\varepsilon} \approx \frac{1}{2}\Delta\varepsilon = \frac{1}{2\varepsilon_0 E}(P_{NL} + i\frac{J_f}{\omega}) = n_2 I - \frac{e^2}{2\varepsilon_0 m}\frac{N_e(r,t)}{(i\frac{\omega}{t} + \omega^2)} \tag{5.2}$$

Also,

$$\left.\begin{aligned} P_{NL} &= \varepsilon_0 \chi^{(3)} |E(\mathrm{r,t})|^2 E(\mathrm{r,t}) \\ (\frac{1}{2}\chi^{(3)} |E|^2 &= n_2 I) \\ J_f(r,\mathrm{t}) &= \frac{e^2}{m}\frac{N_e(r,t)}{(\frac{1}{\tau} - i\omega)}E(r,t) \end{aligned}\right\} \tag{5.3}$$

These last three components are the nonlinear (Kerr) polarization and plasma current $J_f(r,t)$, respectively. Thus, the refractive index change of the medium depends on the laser pulse intensity *I*.

The frequency shift (neglecting the imaginary part) becomes,

$$\Delta\omega \approx (-\frac{\omega}{c} n_2 \frac{dI}{dt} + \frac{e^2}{2\varepsilon_0 cm\omega} \frac{dN_e(r,t)}{dt})L \tag{5.4}$$

The rate of tunnel ionization generating the electron density (N_e) in air in given by

$$\frac{\partial N_e(t)}{\partial t} = W_i(N_0 - N_e) + W_a N_e - aN_e^2 \approx \omega N_0 I^m \tag{5.5}$$

$$W_a = \frac{\sigma I}{U_P} \tag{5.6}$$

$$W_i \approx \sigma_m I^m \tag{5.7}$$

Here, N_0 is the density of neutral air, W_i is the photoionization rate, W_α is the avalanche rate depending on the intensity I and a is the plasma recombination constant. We see that the large frequency blue shift is due to the highly nonlinear dependence on the intensity (m-photon transition). By using a mathematical expression (Perelomov et al., 1966) for W_i (instead of multiphoton ionization rate $W_i = \sigma_m I^m$ with m'th power relation (m = 8)) we find that $\frac{\partial N_e(t)}{\partial t}$ has a positive peak that is much higher than the negative peak. This explains the substantial blueshift $\Delta\omega$ compared to the redshift in the spectra of Figure 5.4. Negative values for $\frac{\partial N_e(t)}{\partial t}$ is permitted if an exact expression of Equation 5.5 is computed without approximation.

Below, in Figure 5.4 shows the spectra of white light (vertical axis is in arbitrary unit) for different average laser powers and lower repetition rate of 500 kHz, generated by the focused spot underwater and taken by the spectrometer connected to a fiber.

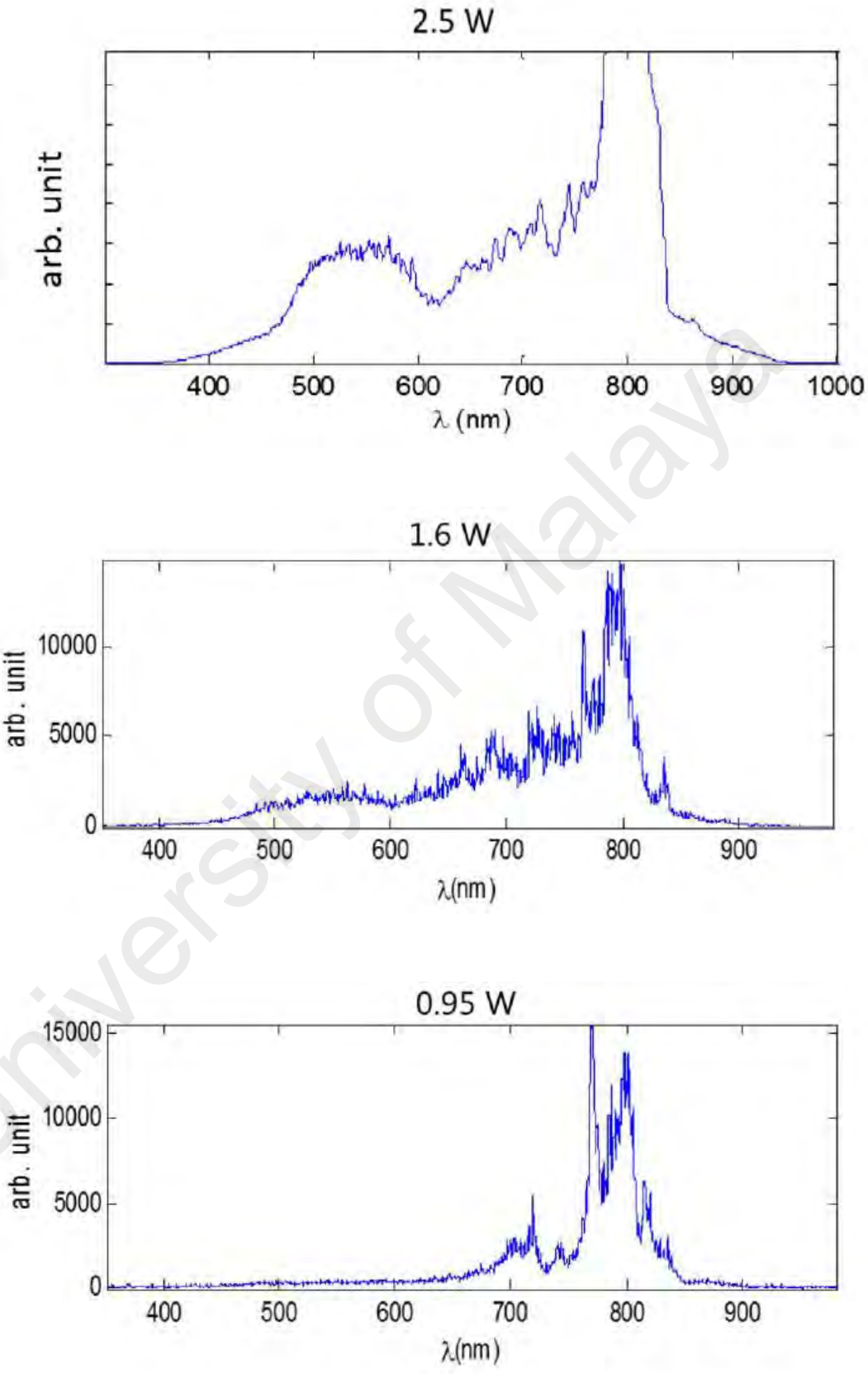

Figure 5.4: Spectroscopic graphs of laser induced plasma inside water.

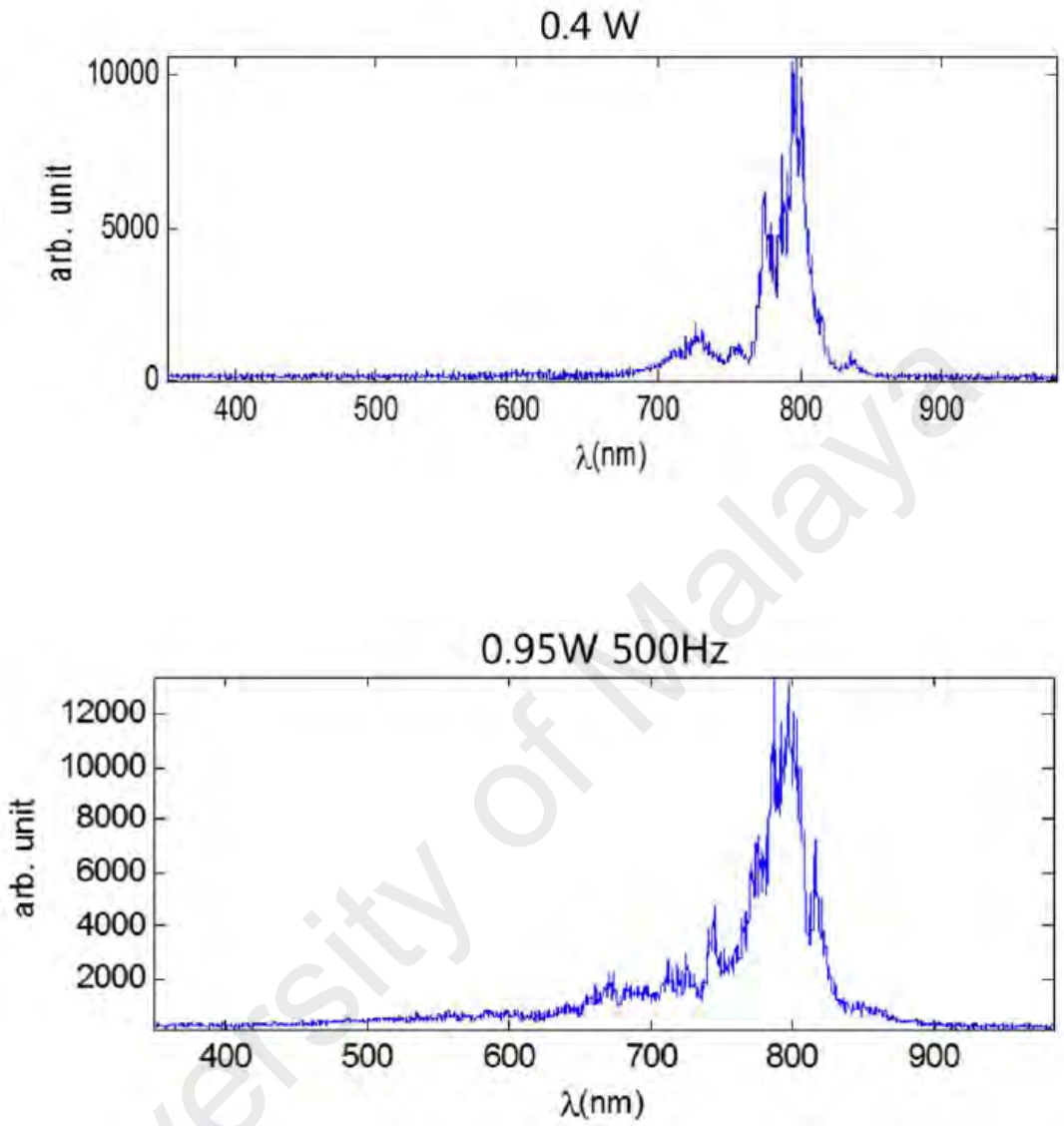

Figure 5.4, Continued.

Observations show that, the focused region glows intensely, emitting a bright white light in the forward direction as the result of supercontinuum generation in water. This is in contrast to the case of focused femtosecond laser in the air (Xu et al., 2014), where colorful scattered image is seen on the screen (Ooi & Talib, 2016) instead of a clear white light. A previous work (Aközbek et al., 2001) predicted that the spectral content in the case of air but it does not reflect on the frequencies distribution on the image plane. The

spectra of the white light generated in the forward direction, the focused laser inside the water, as shown in Figure 5.4. The white light is composed of a broadband spectrum with wavelengths shorter than 800 nm, spanning over the entire visible spectrum, down to ultraviolet 350 nm and up to near infrared 950 nm. Two strong and broad bands around 500 nm and 700 nm overlap are due nonlinear processes, such as Raman and self-phase modulation in the water molecules. At sufficiently high intensity, we find multiple individual peaks within the white light continuum generated by nonlinear mixing processes. However, the peaks may contain spectroscopic lines associated with the water molecules but they are broadband in nature due to the typically large damping in fluidic environment. The dip around 610 nm is also found in other work (Sreeja et al., 2013).

5.3 Creation of Bubbles

The intense laser field near the focus creates intense photoionization, the breaking molecular bonds, generation of plasma and water vapor, leading to water splitting and catastrophic breakdown that manifest into explosive boiling and sporadic creation of bubbles that expand to a stable size. Intense photoionization of water molecules produces mixtures of hydrogen and oxygen ions as nucleation centers for the nanobubbles. After the plasma decays, the recombination energy is converted to boiling water where nonequilibrium phase transformation of the liquid into vapor takes place. Recombining plasma leads to vaporization of water and explosive boiling that creates expanding nanobubbles filled with gas or vapor. Once the nanobubble is created, it rapidly expands outward and radially into microbubble due to the pressure force originating from the ionized gas and pressurized vapor in the bubble. The bubbles that are created with a dimension smaller than about 10 microns were disappearing more quickly as they shrink and then collapse as the pressure force of the smaller bubbles are smaller and can be suppressed by the fluid pressure.

The expansion of nano-bubbles into micro-bubbles is rapid, well below a millisecond. However, this transformation is not ultrafast although it is driven by ultrafast laser pulses. As this work's main focus is not bubble dynamics, therefore, time-resolve technique or study of dynamic processes in materials or chemical compounds by means of spectroscopic techniques were not used here as this work is not focused on the transient optical emission processes of nanobubbles transforming to microbubbles, we discussed the necessary parts of this dynamics relevant to our work. We estimate the timescale of the bubble dynamics by investigating captured video of the laser-water interaction process using a camera (Canon IXUS160) placed on a microscope eyepiece. We analyzed the dynamics and optical emissions was then analyzed by capturing the resulting process into video format, using a commercial video playing software where the speed of the motion picture can be controlled. We find that the motion picture is not resolved faster than a millisecond. Therefore, we may infer the duration of expansion from nanobubble to microbubble as below a millisecond.

5.4 Rapid Generation of Bubbles

We observe the creation of microbubbles in explosive boiling (shown in Figure 5.5), from focused femtosecond laser in the water. These microbubbles serve as the scattering medium which aids in visualisins the hydrodynamic flow of the fluid around the region of focused laser region inside the water. The process was captured in videos and snapshots, showing the motion of bubbles for different laser powers. Typically, the fluid is found to be to wards the focused region. However, at higher intensities (by controlling electronic current larger than 18 A or 1.5 W as Figure 4.2), we observed rapidly running bubbles (RRB) were observed glowing and moving opposite to the laser beam and towards the focus. This is the result of the strong optical force of the focused laser functioning like an optical tweezer. In the region just behind the focus, we notice the violently boiling bubbles (VBB) due to the extreme nonequilibrium water-vapor phase

transition caused by the femtosecond laser pulses at 800 nm, i.e. in the near IR regime. Convective flow of bubbles and stronger explosive boiling mechanisms here result in the removal of mass which converts the water molecules into water vapors. An interesting reason for this occurs here and not at the focus lies in the competing mechanism of plasma formation that generate bubbles and collective white light at the peak intensity.

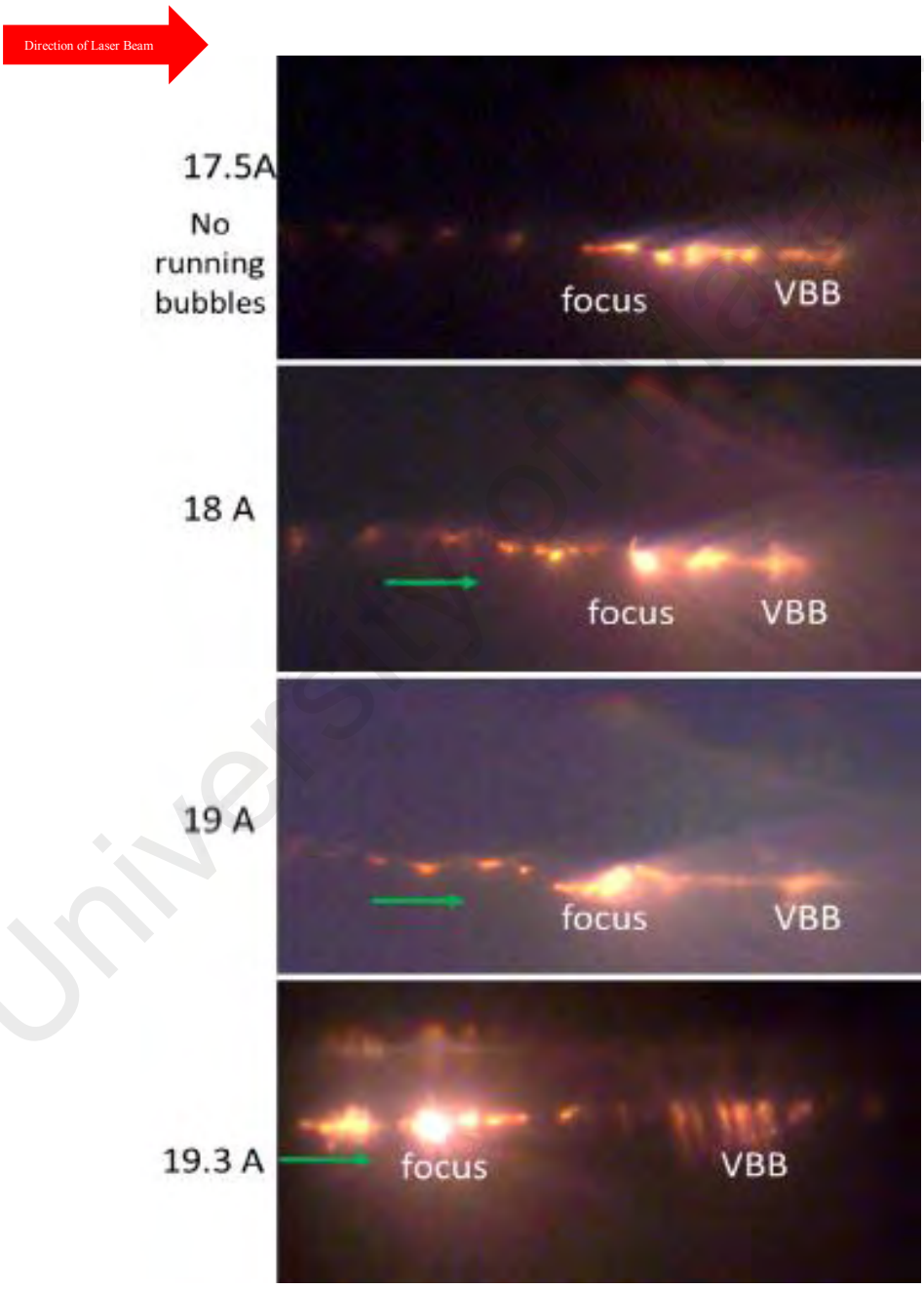

Figure 5.5: Generation of bubbles (side view) for different laser intensity.

As shown in Figure 5.6 violently boiling bubbles (VBB) is found behind the focus while at higher intensity, this rapidly running bubbles (RRB) can be seen moving opposite (green arrow) to the laser beam and towards the focus, with white light emitting in the forward direction for different values of current.

5.5 Colored Light Scattering by Bubbles

At a lower the average laser beam power 0.4 W (corresponding to electronic current of 17A), the bubbles are created sporadically near the focus before showing any colored lights. As the bubbles drift through the light cone of the focused femtosecond laser, they glow for about 0.1 second by emitting colored lights (or white light at high intensity) somewhere inside the conic region of the strong laser field as shown in Figure 5.6. The tiny colored lights are seen only at the back edge of the bubble, at the water-bubble boundary and have an estimated size of about 1 micron using microscope and microscopic software. As clearly shown in Figure 5.7 the fact that the colored lights are seen only within the conic region illuminated by the focused laser proves that these lights are due to scattering by the focused laser.

We analyzed the optical emissions from the bubbles surface using a commercial video playing and editing software Filmora, where the speed of the motion picture can be controlled. Using the software we found 25 images from a single second-time length. So, the time difference of each frame is 0.04 second. This analyzing gave us a very good conception of our observed scattering. It has been found that the new-found phenomena of colored light emissions are actually due to scattering at the surface of the bubbles after the focused femtosecond laser undergoes nonlinear interactions and filamentations in the water. In contrast to recent works on microbubbles, the light emission here does not occur at the geometrical center of the bubble (Sankin et al., 2005; Liu et al., 2016), but at the back spot/edge facing the incoming laser as displayed Figure 5.7. The colored lights are

blue-shifted by nonlinear interactions (described in the following subsection) while the consistent light-emission point at the backside of the bubbles is due to scattering/reflection of lights from the filamentation hot spots of different spectral components assisted by self-focusing. According to Fresnel reflection, the electric field at the backside interface is $E_0(\frac{2n_1}{n_2+n_1})$ i.e., the sum of the incident and reflected fields, is enhanced by11% taking n_1=1.33 in water and n_2=1 in the air (Crisp et al., 1972).

Figure 5.6: Sparkling color lights and dark bubbles.

The physics of the colored filaments was described in ref (Hao et al., 2011) as due to the filaments having different degrees of nonlinearity, self-focusing, SPM, and multiphoton ionization (plasma defocusing), as well as different laser intensities at different positions, leading to different degrees of spectral broadening (Figure 5.9). For peak power of 8 GW, the number of filaments is estimated to be (Couairon & Mysyrowicz, 2007),

$$N \approx P_{in} / P_{fil} = \frac{P_{in}}{(\pi/2)^2 (\lambda^2 / 2\pi n_0 n_2)} = \frac{8\times10^9 W \times 2\pi \frac{4}{3} \times 26\times10^{-21} m^2/W}{(\pi/2)^2 (800nm)^2} = 1103 \quad (5.7)$$

Where, P_{in} is the average laser power, P_{fil} is the power carried by each filament and we use $n_2 = 26 \times 10^{-21} m^2/W$

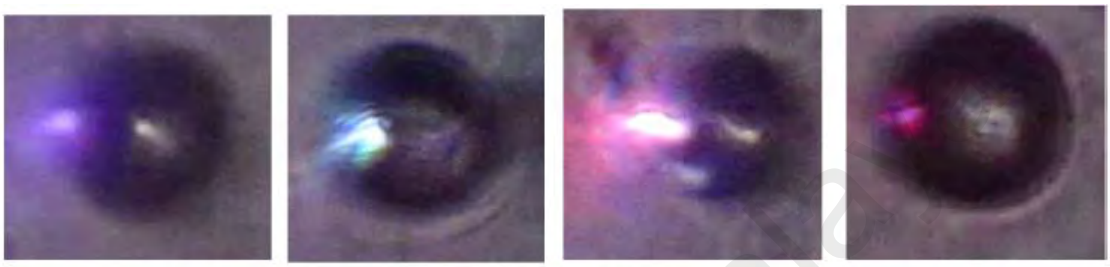

Figure 5.7: Color light scattering by single bubbles.

The scattering of supercontinuum at the formed bubble surfaces does identify the "hotspots" due to filamentation where the intensity is high but is not directly observable at points lateral to the propagation direction and outside the scattering cone. The bubbles, created by the hot spots where photoionization is strong enough to cause molecular disintegration and nucleation of bubbles, act as scattering medium to illuminate those hot spots. Thus, the hot spots are not necessarily the spots where the bubbles are created (referred to as hotter spots) and may be best illustrated by the bright regions in Figure 5.9 for the case of focusing into the air. The supercontinuum (white light) generated at the "hotspot" can be seen (in Figure. 5.4) to propagate through the water for large distances away from the hotspot because it is scattered by the water since there are no bubbles in the water except near the focusing region. The following observations further support our explanation of the phenomena. The high (1kHz) repetition rate of the laser means that the bubbles are almost continuously illuminated within a fixed focused (conical) region in the water instead of just a single pulse excitation. But the colored lights are emitted as sparks and not continuous. Only at certain fixed locations, the bubbles come into contact

with the hot spots where strong colored lights at blue-shifted frequencies are optically scattered at the water-vapor interface of the bubbles. This shows the presence of hot spots due to filamentations. The convex surface of the spherical bubbles enables us to see the scattered/reflected colored lights at a finite range of observation angles/directions. As the bubbles move, the intensity and the colored of the scattered lights change. At times, the white glow can be seen at the same back side of each bubble, an effect due to strong self-phase modulation.

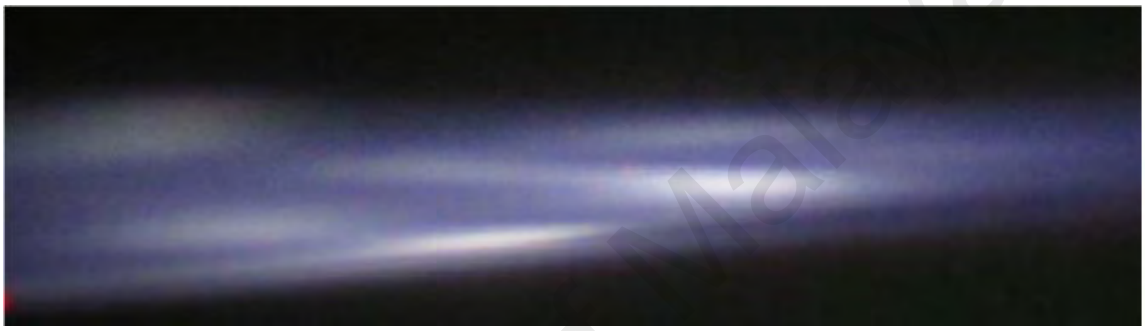

Figure 5.8: Multi filaments by focused femtosecond laser in air.

After emitting the lights, the bubbles do not show any sign of collapse, thus there is no sonoluminescence here. The analyzed clips (Figure 5.9) clearly show the bubbles drift continuously and do not show any collapse or sudden disappearance, unlike the case of bubble sonoluminescence usually created by the ultrasonic method or weaker laser excitation.

The bubbles in the regions outside the scope of the laser field appear dark and quite stable, with only a tiny bright spot at the center under the illumination of the halogen light of the microscope from above. This is typical when a transparent microsphere is not scattered by the laser light.

At high electronic current 19A (average laser beam power 2.7 W), it seems that the colored lights are emitted prior to the formation of bubbles. This is because the laser field

is so intense that the scattering effect is so strong that it overshadows the formation of bubbles.

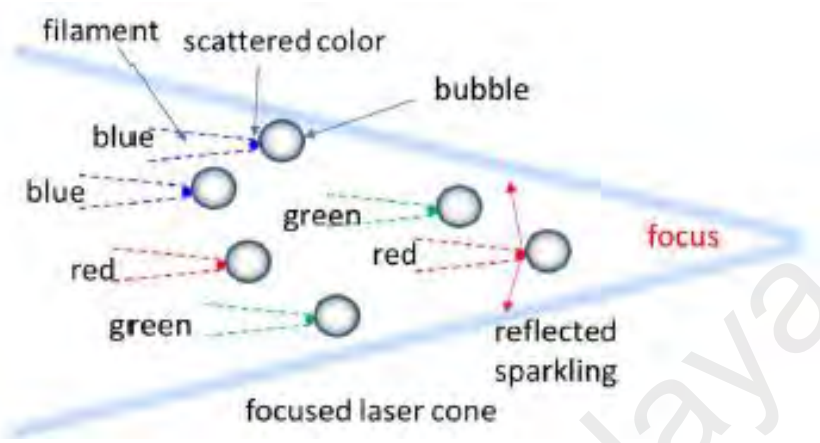

Figure 5.9: Multi filaments by focused femtosecond laser in air.

However, a closer look at the motion pictures in the video camera at lower power (current 16.4 A) reveals that the cluster of bubbles are always created before we see the sparkling colored lights. As an evidence below, a sequence of analyzed video snaps are attached with an analytical explanation in Figure 5.10. Besides, some additional observational informative decision will be found in section 5.7.

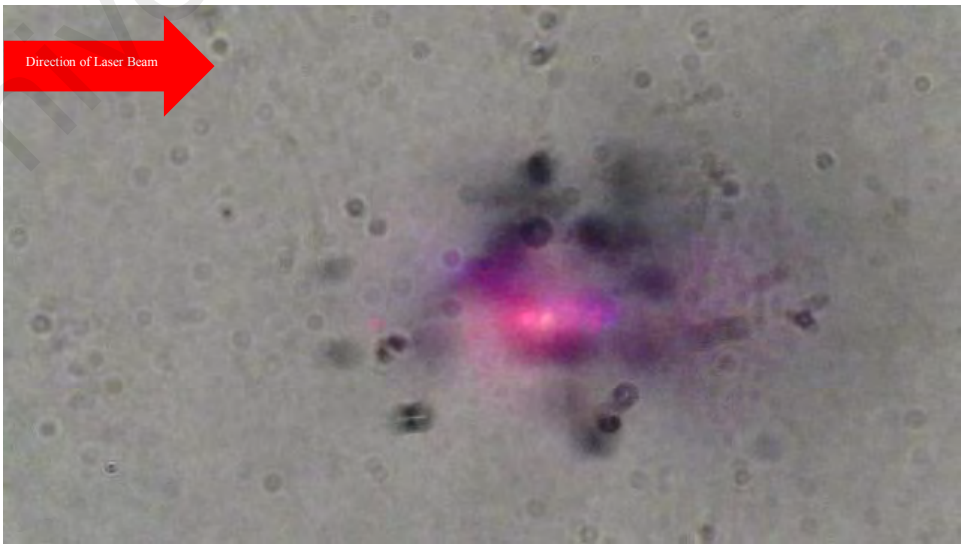

Time = 0.00 s

Figure 5.10: Bubbles movement and scattering of color light within 0.48 second.

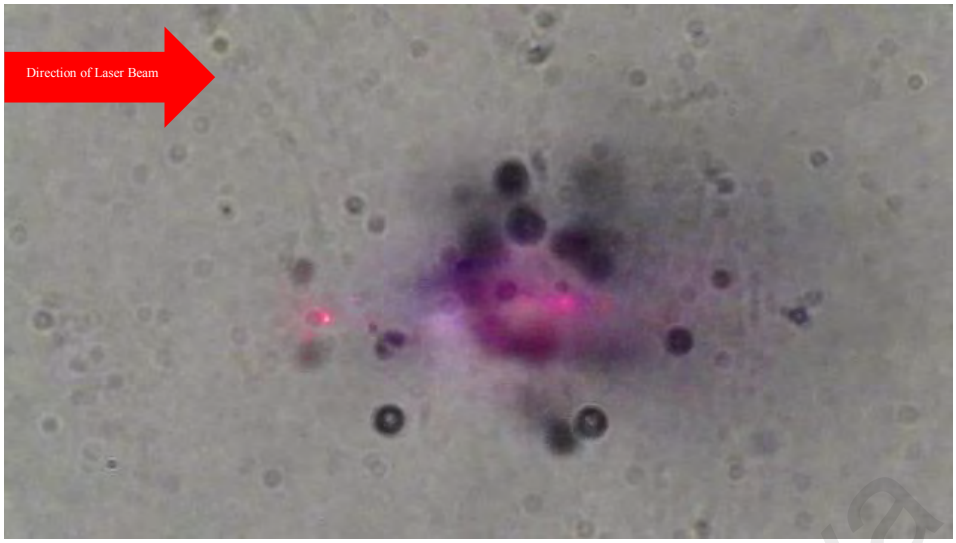

Time = 0.04 s

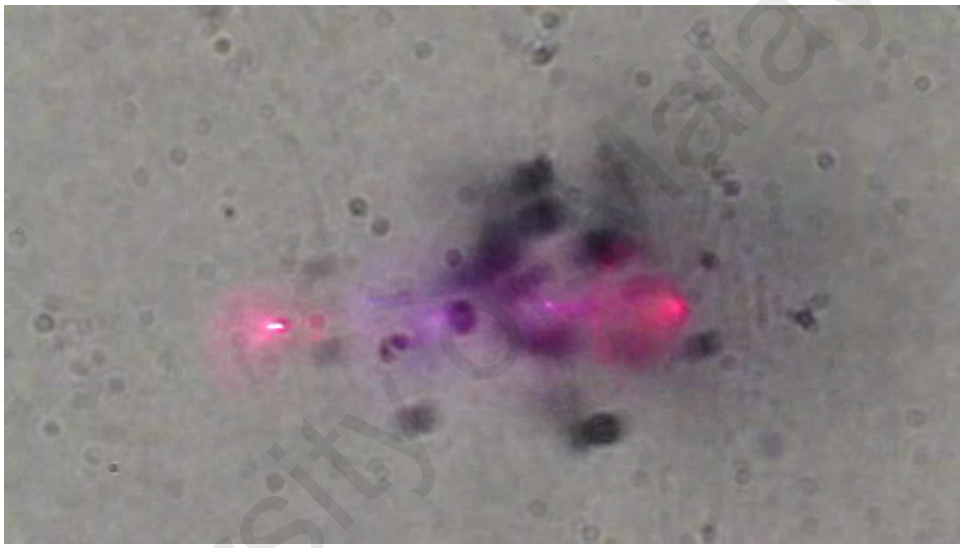

Time = 0.08 s

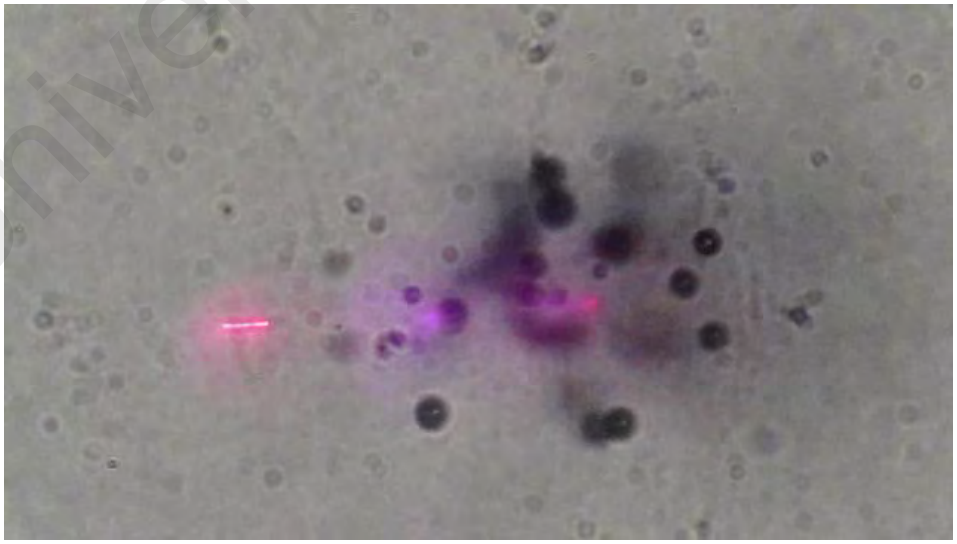

Time = 0.12 s

Figure 5.10, Continued.

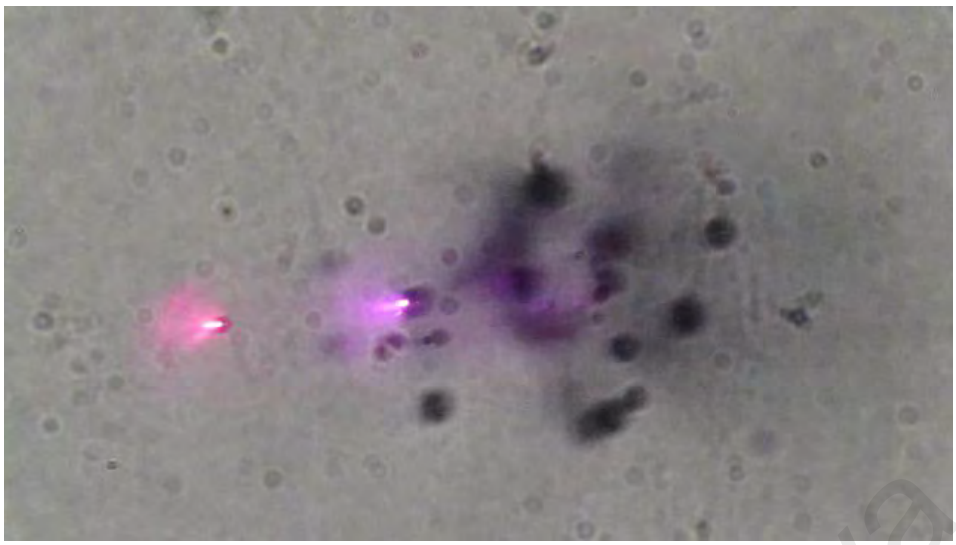

Time = 0.16 s

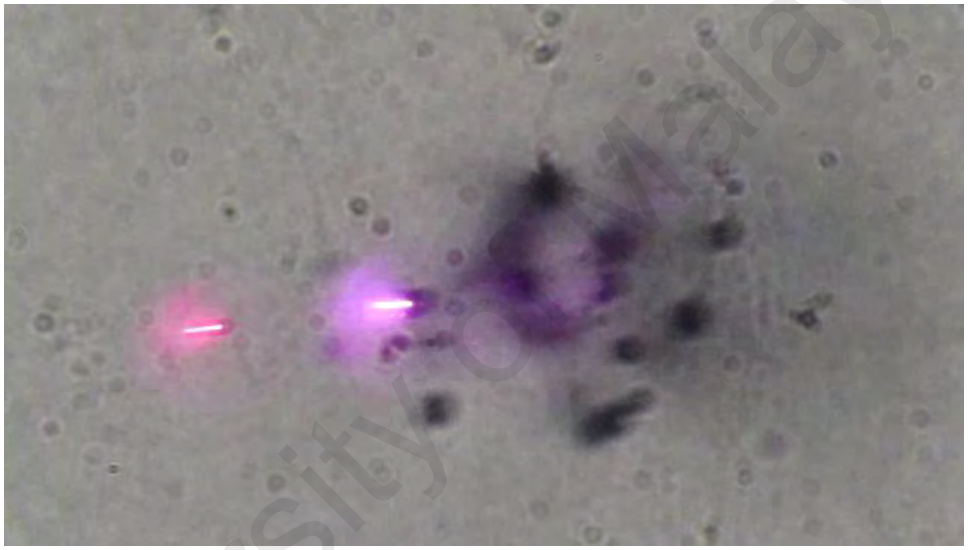

Time = 0.20 s

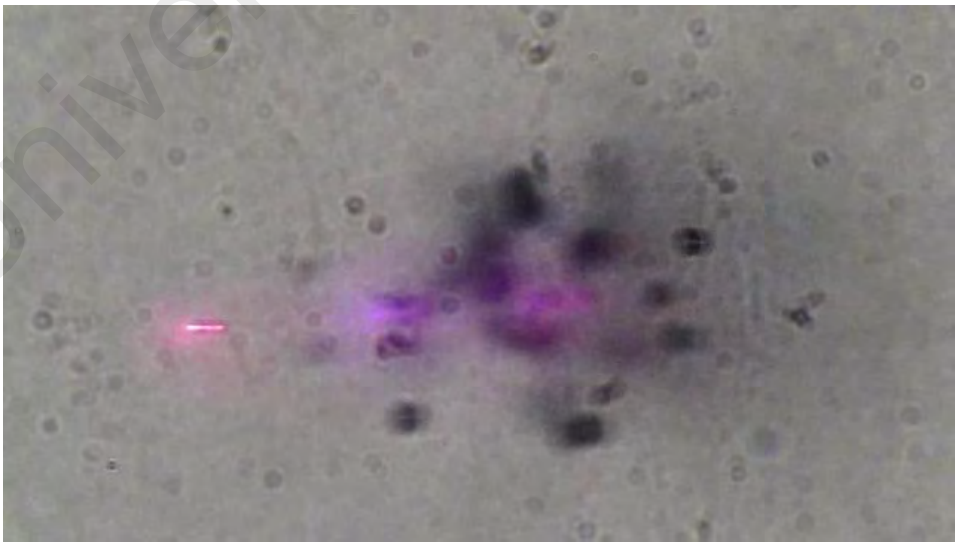

Time = 0.24 s

Figure 5.10, Continued.

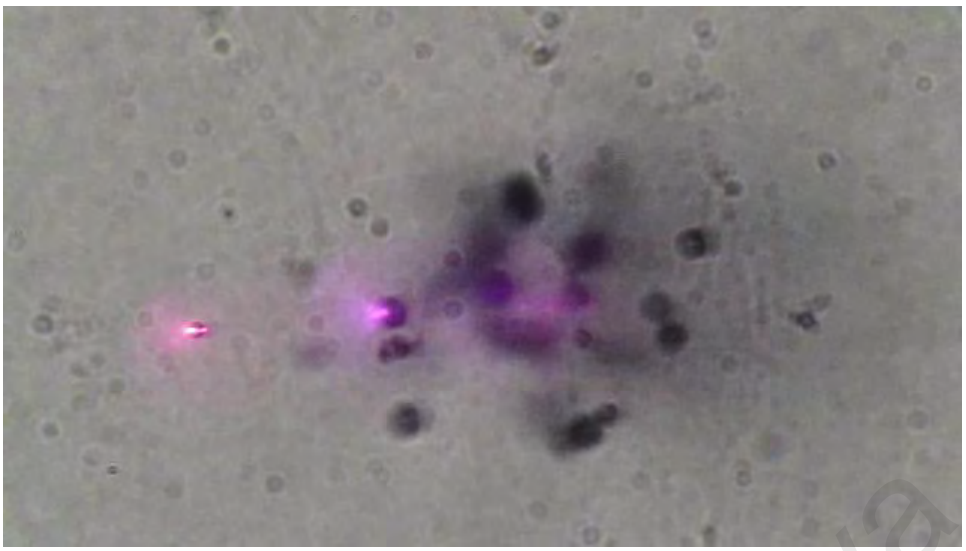

Time = 0.28 s

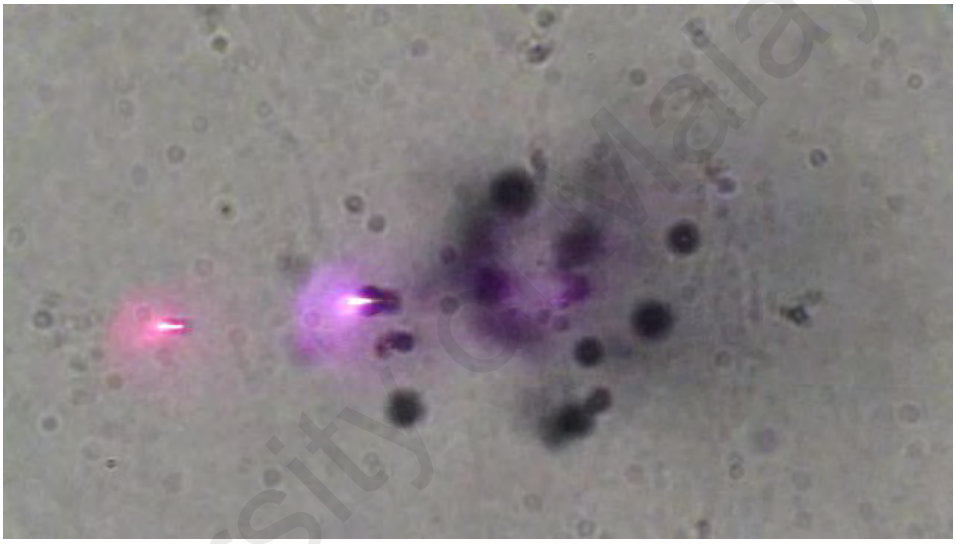

Time = 0.32 s

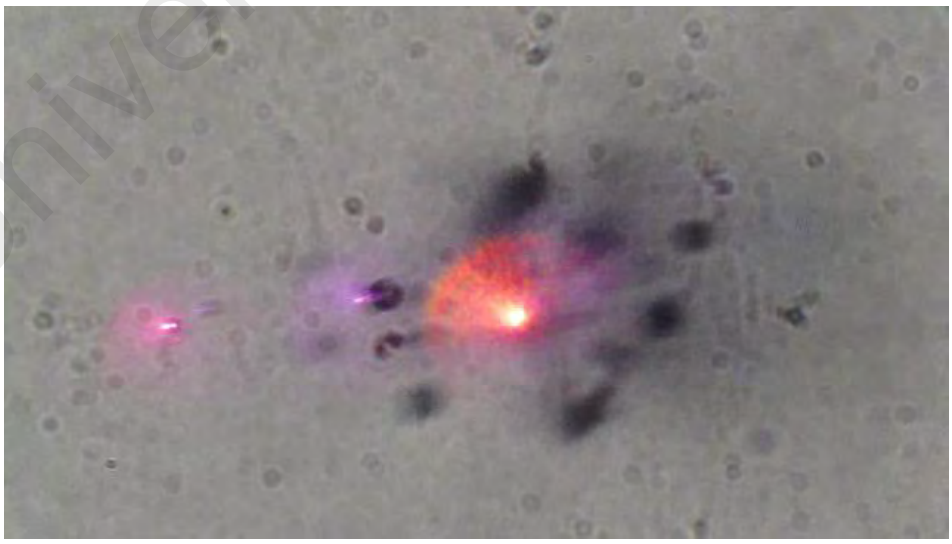

Time = 0.36 s

Figure 5.10, Continued.

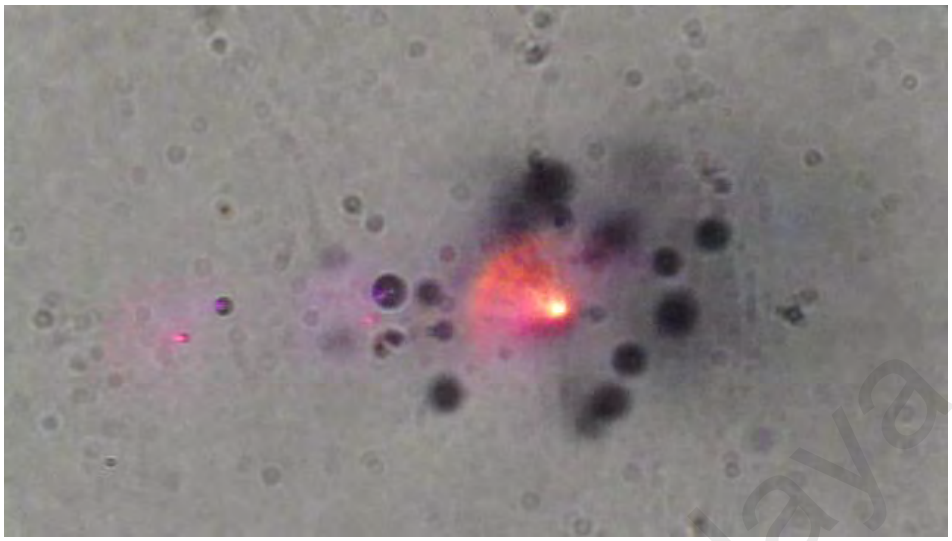

Time = 0.40 s

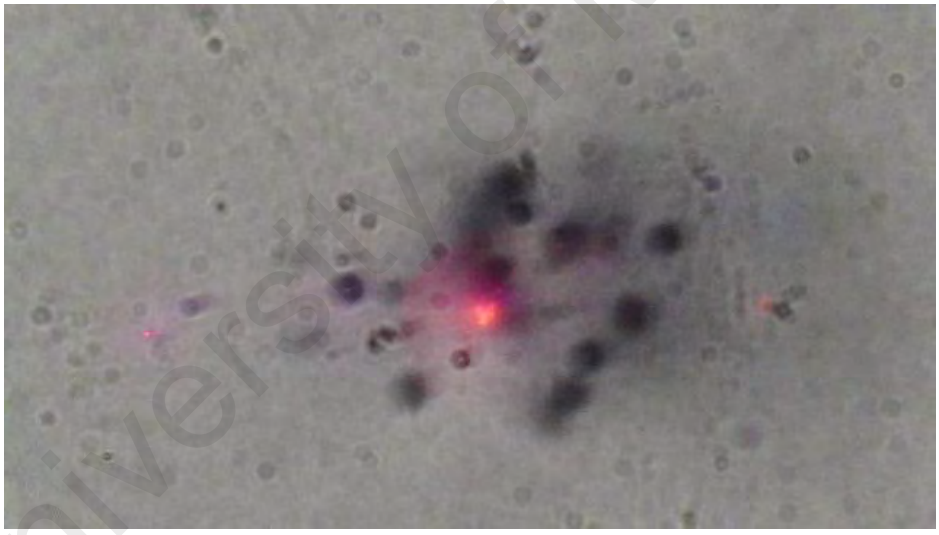

Time = 0.42 s

Figure 5.10, Continued.

This sequence of pictures can describe the basic finding in brief. These images are analyzed from 0.48 second of a captured video clip. At first, we see the first image was captured at zero seconds then each frame has been taken with the time difference of 0.04 second. In first image an unfocused colorful region, this region is not in the layer of our

focusing point through the microscope, in following next image it has clearly seen that one bubble with red scattering color is moving left side toward laser, when the laser was focused from left side (Figure 5.10).

In this picture is clear that bubbles are generating spontaneously, the dense but blur part of the images are representing focus region by laser but plasma is not visible because it is not in the focus point. A red light scattering bubble was always there since time frame 0.02 s, and was moving more leftward (which is the directing from where laser was coming in). At time frame 0.20 s a blue color scattering bubble gets attention for its visibility, it's almost double in size compare to red sparking bubble. After 0.38 s both blue and red color scattering bubbles gradually disappear. This due to upward direction of the bobbles, and at 0.42 it has seen those bubbles are completely disappeared by going out of focus.

5.6 Approximate Position and Size Distribution of Scattering Color Bubbles

In the early of this chapter it is mentioned this experiment is based on microscopic level observations, to do so a lot of precise recording, imaging and analysis were required during analysis. Some graphical representations were also performed by taking data when scattering lights were showing highest level of brightness. Figure 5.11 represent those data. Most of the bright sparks were in red, yellow, green, blue-violet, and violate color. And all were taken from four video clips, chronologically their durations are 47 s, 3 min 21 s, 2 min 08 s and 29 s. The graphical units are abstract values, furthermore represented x and y axis also do not exist. A clear view of the total position of all the pick scattering will be found in scatter plot of Figure 5.13.

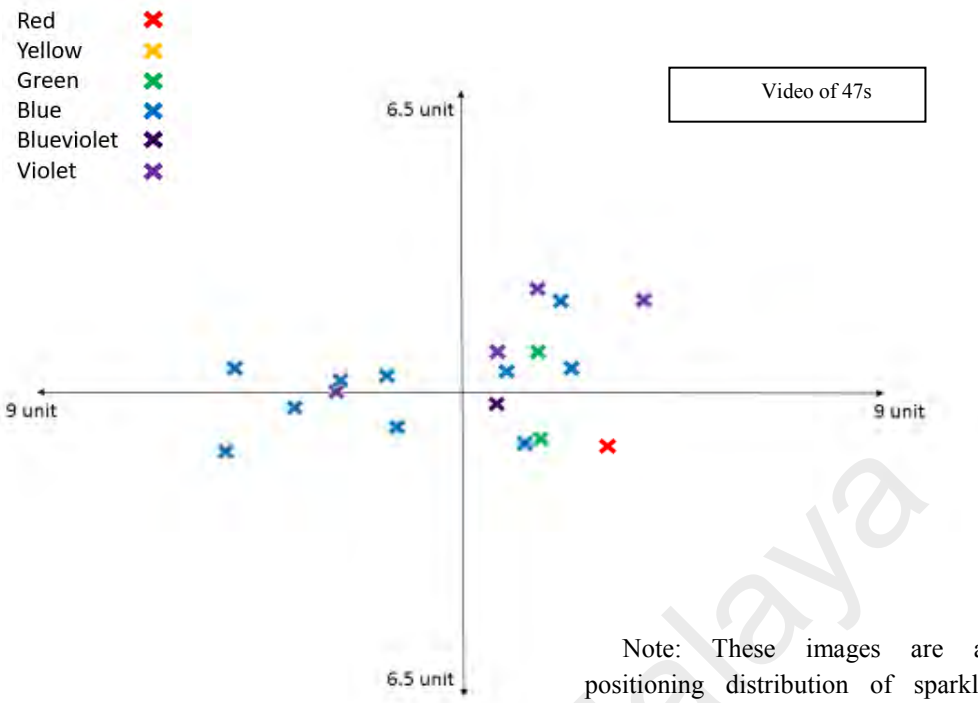

Note: These images are abstract positioning distribution of sparkling of bubbles surface based on similar images of each video sections found in Figure 5.10. So no scaling is required. Each crosses are representing each colors of brightest sparking.

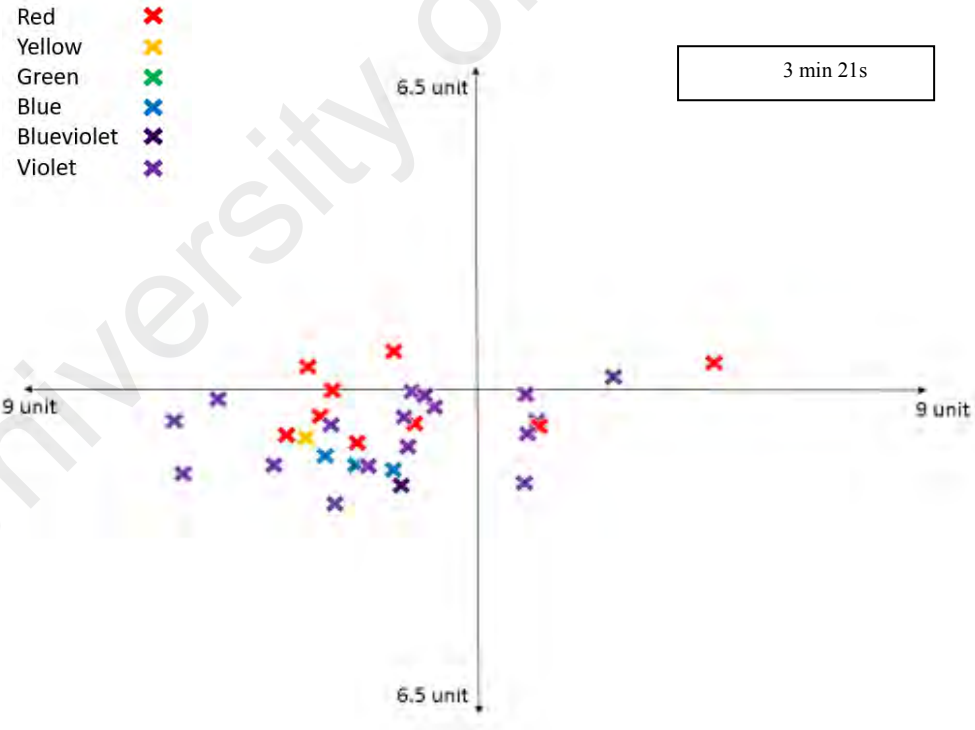

Figure 5.11: Position distribution during brightest spark.

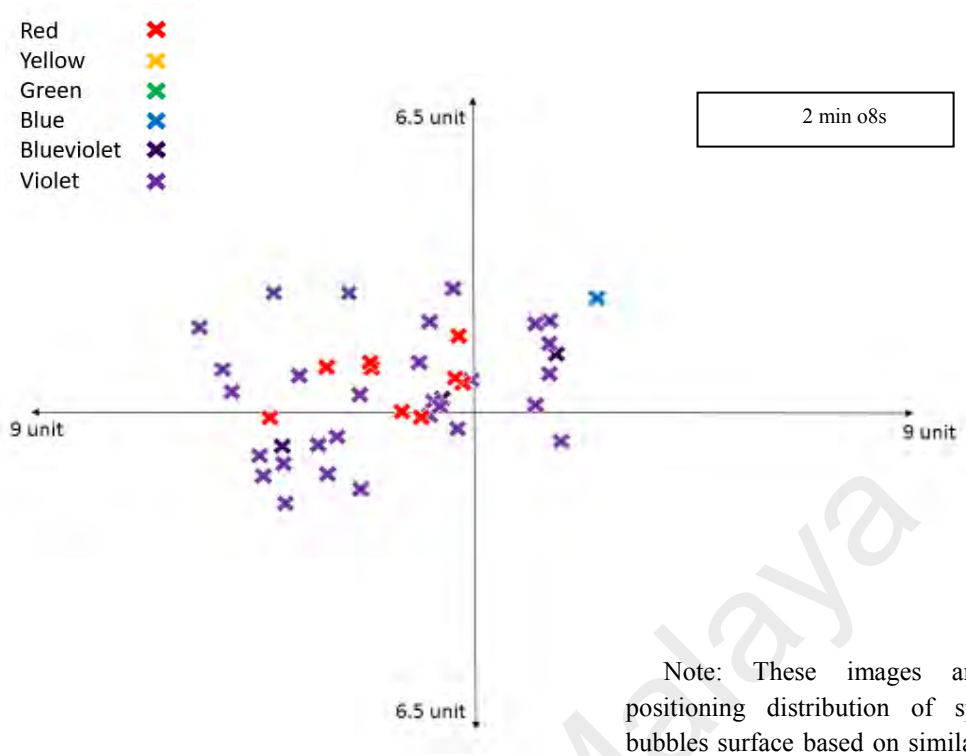

Note: These images are abstract positioning distribution of sparkling of bubbles surface based on similar images of each video sections found in Figure 5.10. So no scaling is required. Each crosses are representing each colors of brightest sparking.

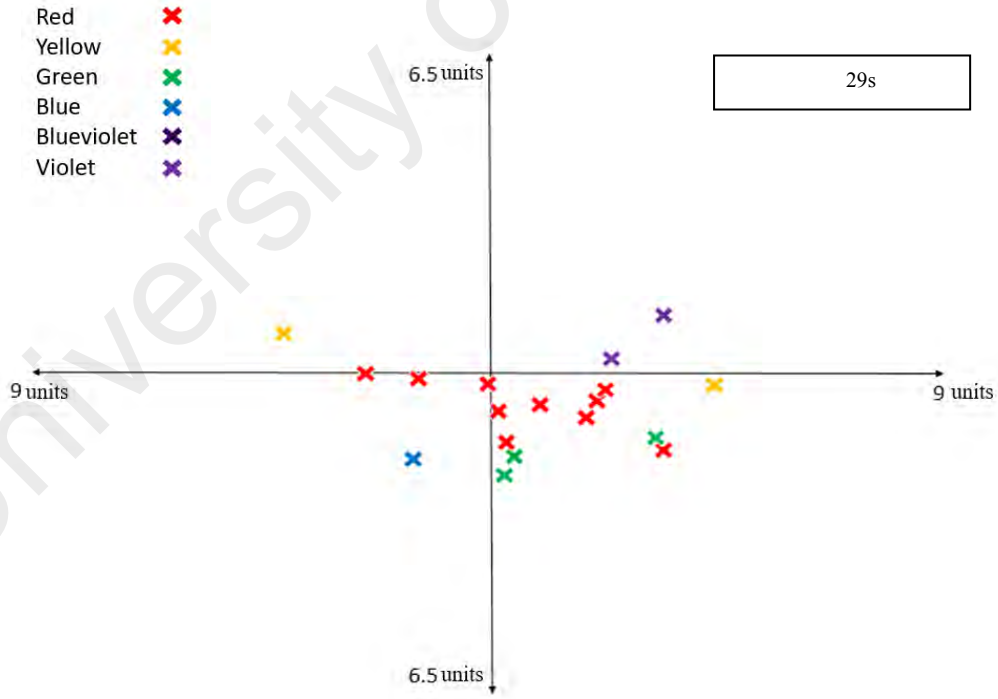

Figure 5.11, Continued.

So from the images, we can clearly see violate color sparking was a higher amount, the second higher amount is red, third is blue and then rest.

However, Figure 5.11 does not show any size and color relation of our observations. To see the relationship we have created Figure 5.12 of four plots by those four video clips, where each cross with color represents each color bubbles, and diameter of bubbles are also representing in a graphical way.

Below colors and size of bubbles are also mentioned.

Table 5.1: Scattering color and bubble diameter size distribution from different video clips.

Video Clip Number	Video Clip Duration	Red	Yellow	Green	Blue	Blue Violate	Violet
1	47s	25		15, 20, 20	20, 13, 20, 20, 19, 20	22, 19, 20	19, 25, 20
2	3 min 21s	30, 20, 20, 25, 20, 15, 18, 17, 30	20		18,20	20	20, 20, 13, 20, 20, 19, 20, 21, 10, 15, 18, 20, 30, 10, 10, 21
3	2 min 08 s	30 , 17, 18, 20, 20, 20, 30, 22, 25			22		20, 20, 20, 20, 20, 18, 20, 21, 25, 22, 20, 18, 17, 13, 23, 20, 18, 15, 15, 20, 25, 26, 20, 15, 30, 22, 20, 18, 20, 23
4	29 s	25, 20, 21, 23, 18, 21, 20, 20, 25, 22	15,22	20, 20, 22	18	24, 20, 21	25.30

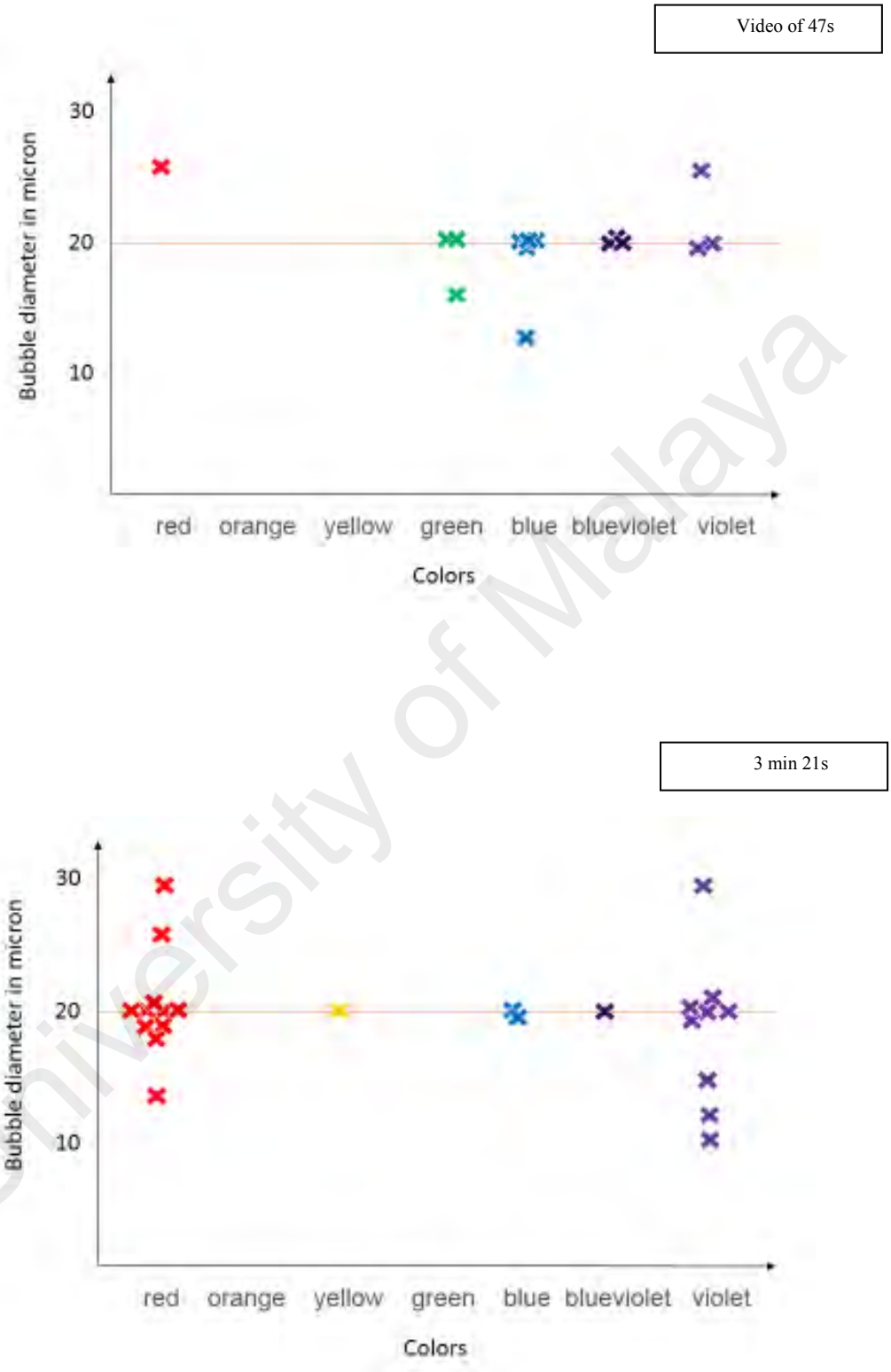

Figure 5.12: Bubble diameter and color distribution.

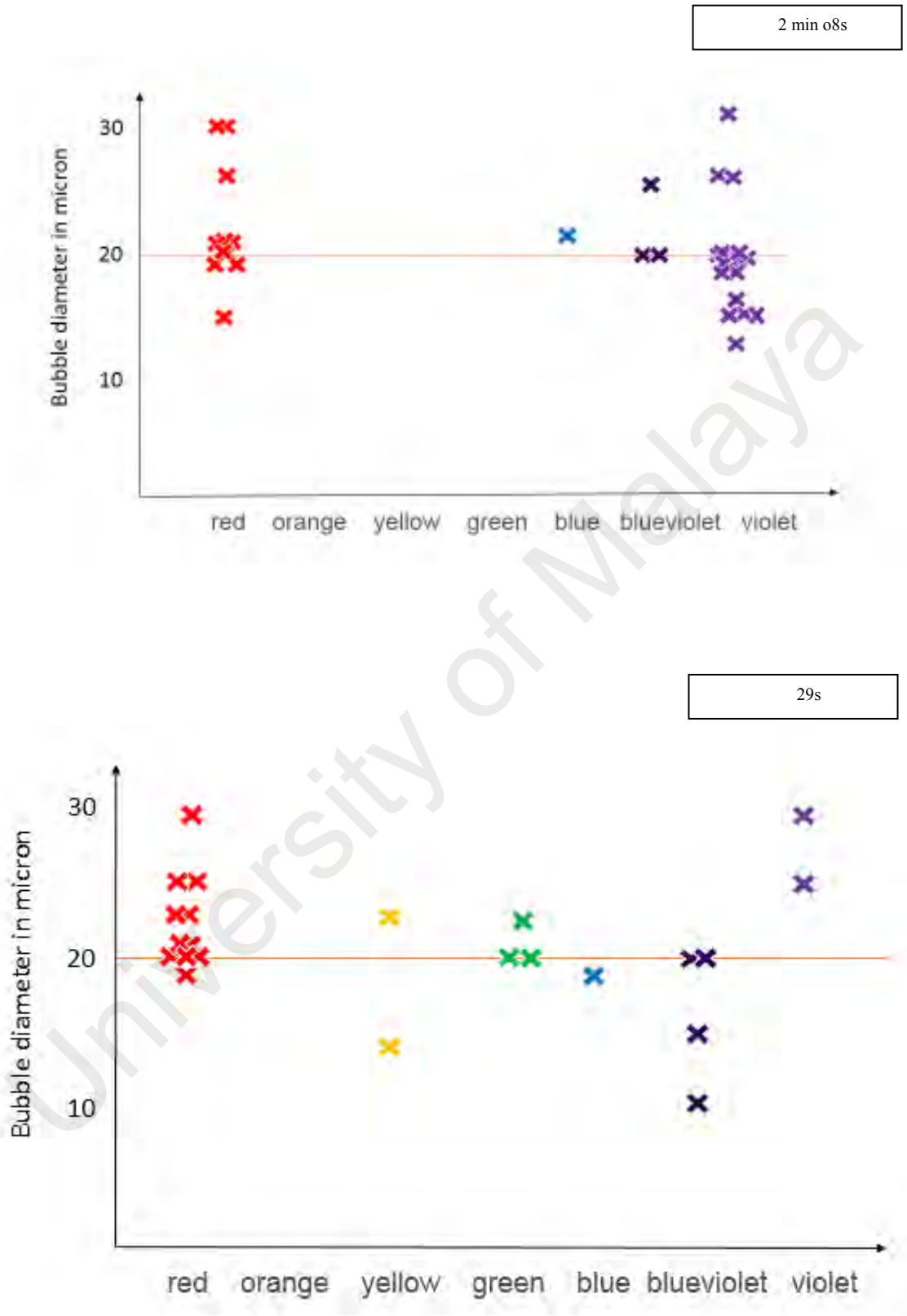

Figure 5.12, Continued.

Collected data and their graphical representations leads us to the answer of the question - Are the colors correlated with space and bubble size? In the finding, it is interesting to note that the distribution of blue dots is more spatially (radially) confined, but the red dots are everywhere as shown in Figure 5.13.

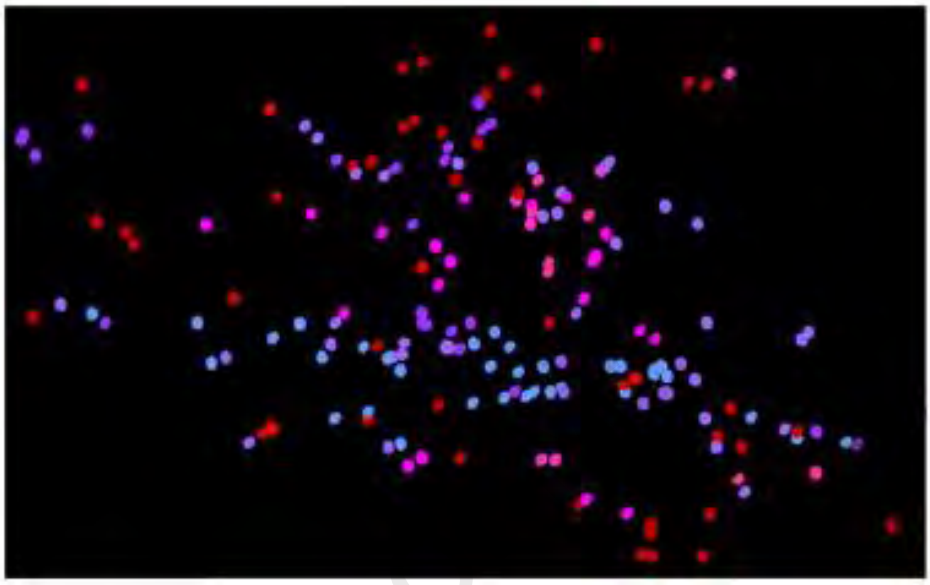

Figure 5.13: Scatter plot of the spatial distributions of the sparkling colors.

It was also observed that the bubbles can emit different colors without changing their size, mainly from pink to blue to red sequentially as they drift along. The mean values of the diameter of the bubbles that emit each color are almost the same based on the histogram of Figure 5.14.

The overall distribution has a mean diameter of 21 μm and variance 32.7 μm, and it does not have a Gaussian fit (Figure 5.15) as we only measure the sparkling bubbles (which are limited in number) are observed. Since the ranges of bubble diameter for the different colors are the same and they all have large variances, we deduce that the colorful emissions have nothing to do with the bubble size, i.e., there is no correlation between color and diameter. The bubble size does not determine which color it would emit. This

rules out the possibility that the colored emission might be due to surface plasmon resonance, as in the case of metallic nanoparticles.

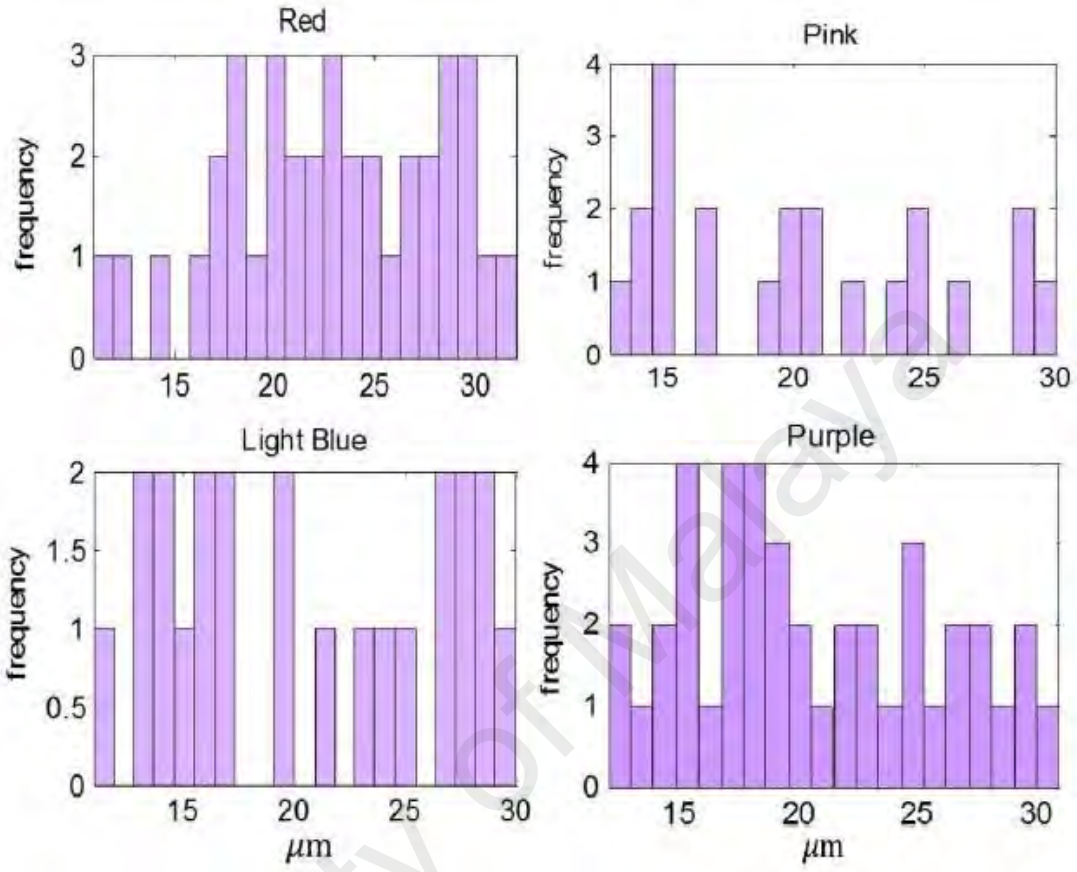

Figure 5.14: Distributions of the bubble diameters for each color.

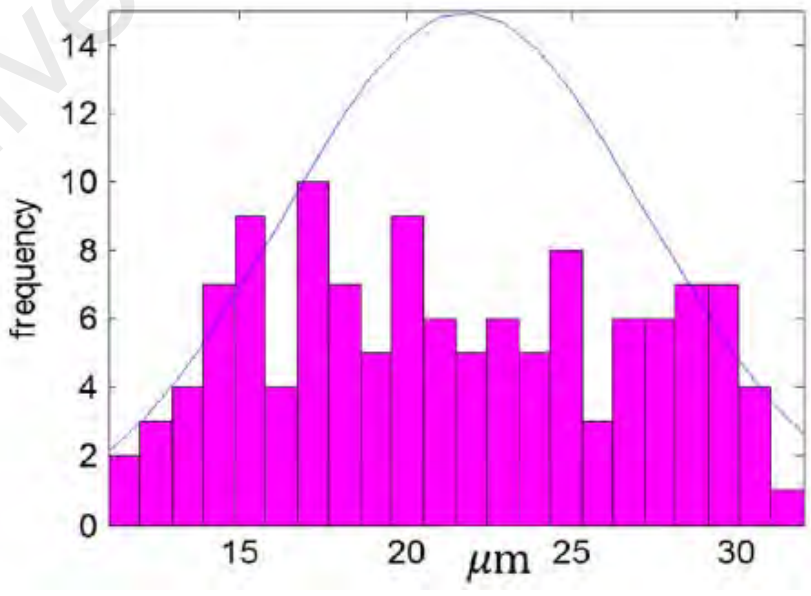

Figure 5.15: Overall distribution of bubbles with all colors and a Gaussian fit.

5.7 Laser power Effect of Multi Spectral Colors

In this experiment the supercontinuum white light was seen along the propagation axis, as it propagates through the water. The white light is created by nonlinear interactions with water as well as scattering by the bubbles near the focusing region. Below the experimental picture shows that the images along the propagation axis at low powers have distinct multiple colors, spatially segregated and inhomogeneously distributed instead of white light. Since there is hardly any bubble at low intensity, we can conclude that the multispectral phenomena of the sparkling bubbles (at higher intensity) is due to nonlinear interactions of the laser pulses with water. At higher power, the white light observed is due to dense overlap of this multiple colors and not due to the bubbles since bubbles merely scatter the sparkling lights at the backward direction and to the transverse direction, not in the forward direction. As the power increases, the colors become more mixed up and the image becomes more blurry, homogeneous and whiter. A different repetition rate affects the details of the image and can only be discerned at low power.

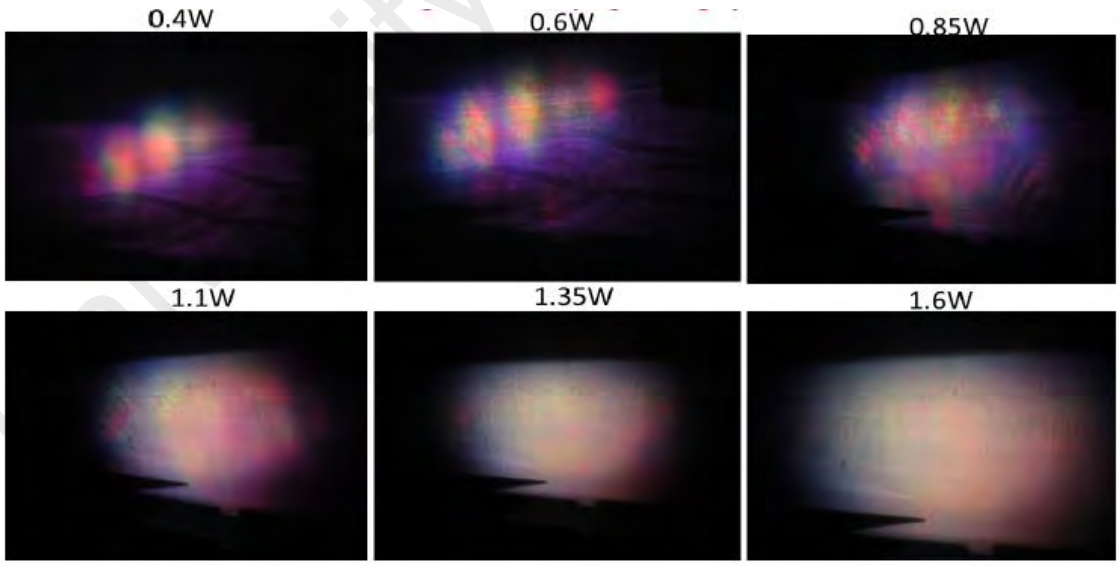

a) White light with varying average power at 1 kHz.

Figure 5.16: Unfocused color and vibrant motion.

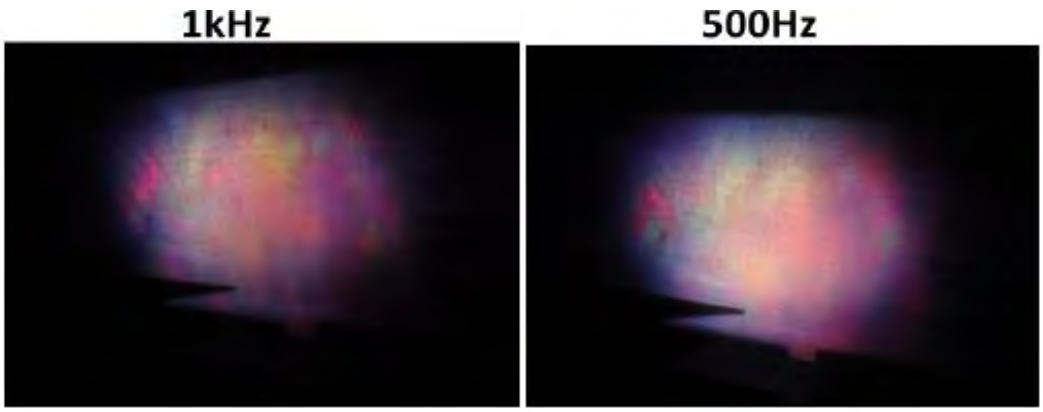

b) Varying reputation rate with 0.95W

Figure 5.16, Continued.

The above multispectral images were taken at the laser axis 1 m away from the focus after the laser passes through the water due to nonlinear optical interactions for different average laser powers. It also shows the colorful image comes at low power and the effect of lower repetition rate of 500 kHz (Raymond & Sanny, 2017).

5.8 The Forces on Bubbles

While observing the optical phenomena of the bubbles, the dynamics of the moving bubbles we also observed. The microbubbles confined within the laser field would drift rapidly toward the direction of the high-intensity region, i.e. the focus, with a speed of 300 μm per second (estimated from scope diameter of 265 micro meters at 40X traversed by bubbles within about 4/3 s).

The pressure force is the main mechanism that drives the moving bubbles. The force is strong around the focus where shock wave creates a depression channel with cavitation/boiling bubbles on the laser axis convecting upward and attracted toward the focus. Similarly, on the other side of the focus, the force is anti-parallel and towards the focus. Near the focus, the bubbles (with larger sizes) are moving/convecting upward

creating the region of depression and the attractive force. This mechanism is well-known (Potemkin et al., 2014) but there is also a gradient force of focused laser on the bubbles that are less well studied and therefore also worth describing here, in addition to the pressure force.

The bubbles are subjected to a strong optical force of the laser field that attracts the bubbles as dielectric particles and has been observed in reference (Liu et al., 2016). However, those bubbles near the edges of the light cone that can overcome the weaker light force of the laser would slowly drift upward while expanding slowly to about 30 microns in diameter.

The study of optical force (Unger & Marston, 1988) and the dynamics of the bubbles require careful theoretical work (Wright et al., 1994) that is beyond the present scope of this work. We are working on the theory of nonlinear optical scattering and the results will be reported elsewhere. However, based on existing theory (Chen et al., 2009; Agayan et al., 2002) we can provide some estimated numbers. The resulting attractive laser force is given by (Unger & Marston, 1988)

$$F_l = I\pi n a^2 Q / c \tag{5.8}$$

It can be noted that this is due to the lower refractive index of the bubble as a scattering particle, contrary to the usual dielectric particle (Z) (Chen et al., 2004), where it can be recalled that buoyancy force $F_b = \frac{4\pi a^2}{3} g(\rho_w - \rho_{air})$, here ρ represents density of water and air respectively, g is gravitational acceleration. Near the laser focus of radius 35 μm, the average power of P_{av} = 0.4W (with repetition rate 1 kHz and peak power 8 GW, pulse peak intensity 2×10^{14} W/cm^2) , the corresponding average intensity is I = 104 Wcm^2.

Using the bubble radius = 10 μm, the efficiency factor for radiation pressure $Q = 0.1914$, the refractive index of water $n = 4/3$ the estimated laser force is 27 pN.

According to the Stokes law, the drag force is,

$$F_d = 6\pi\eta a v \tag{5.9}$$

Which gives 50 pN (pico Newton), using dynamic viscosity of water $\eta = 8.9 \times 10^{-4}$ $kgm^{-1}s^{-1}$, the bubble radius a is 10 μm and velocity v is 300 micro meter per second.

Thus, the larger laser force provides a net force that accelerates the bubbles toward the focus. Thus, the pressure force driven by the convection of the bubbles must be at least larger than the sum of the viscous force F_d = 50pN and the laser force F_l = 27 pN (that repels the bubbles from the strong field region) to provide the net force that accelerates the bubbles toward the focus region.

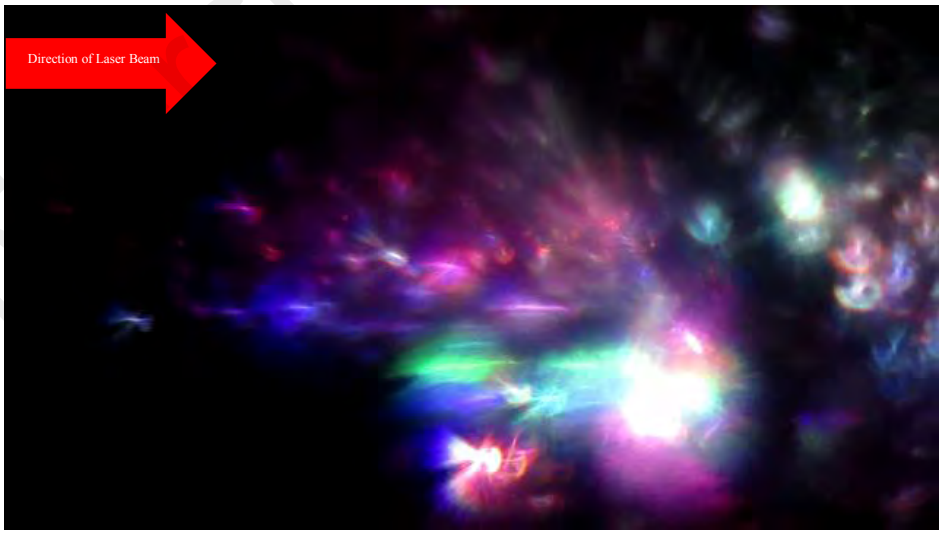

Time = 0.00 s

Figure 5.17: Unfocused color and vibrant motion.

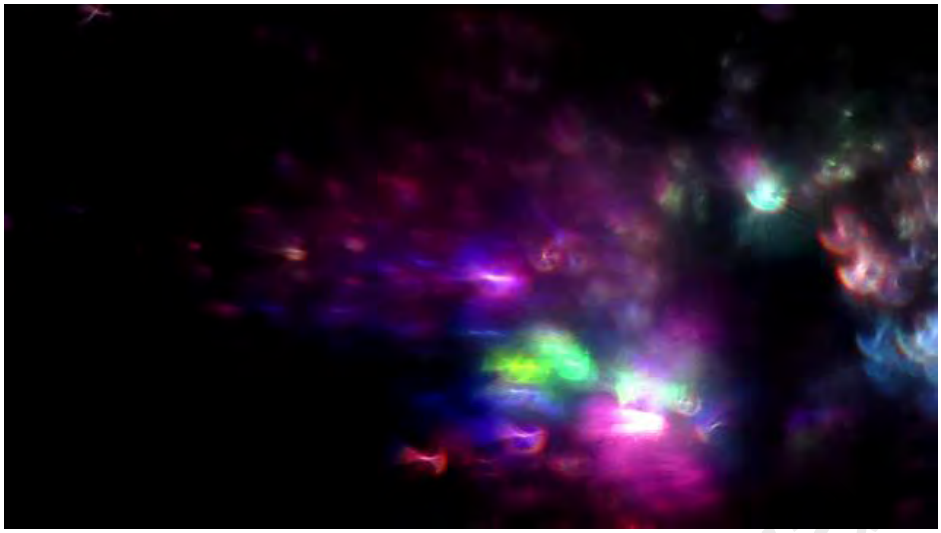

Time = 0.04 s

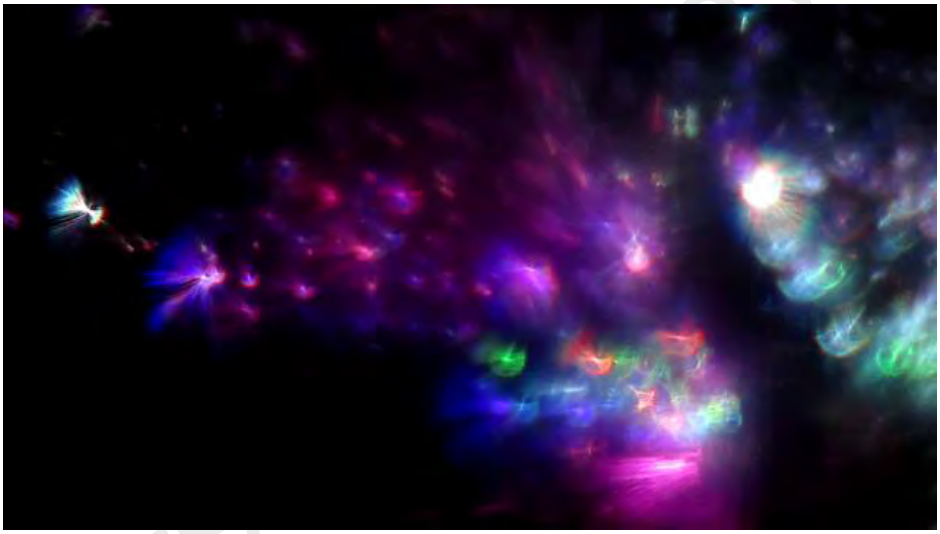

Time = 0.08 s

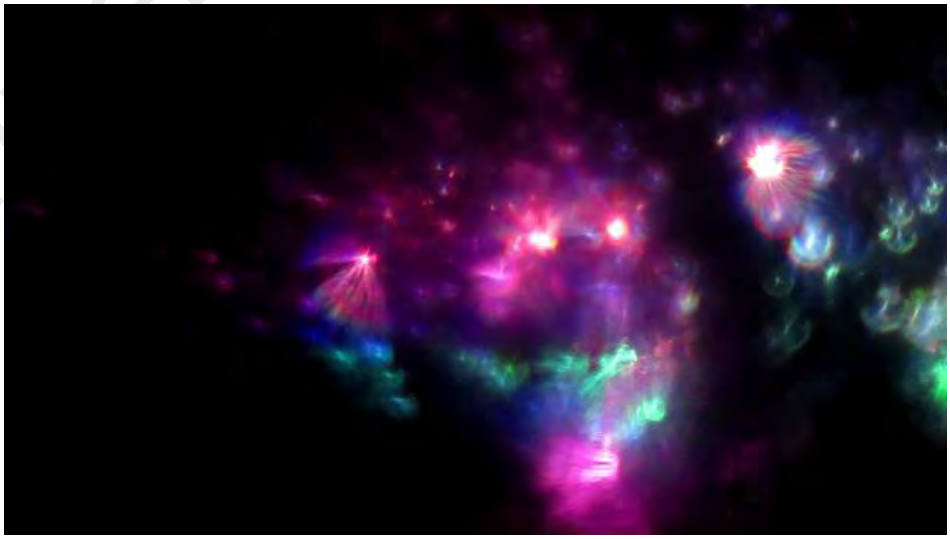

Time = 0.12 s

Figure 5.17, Continued.

Time = 0.16 s

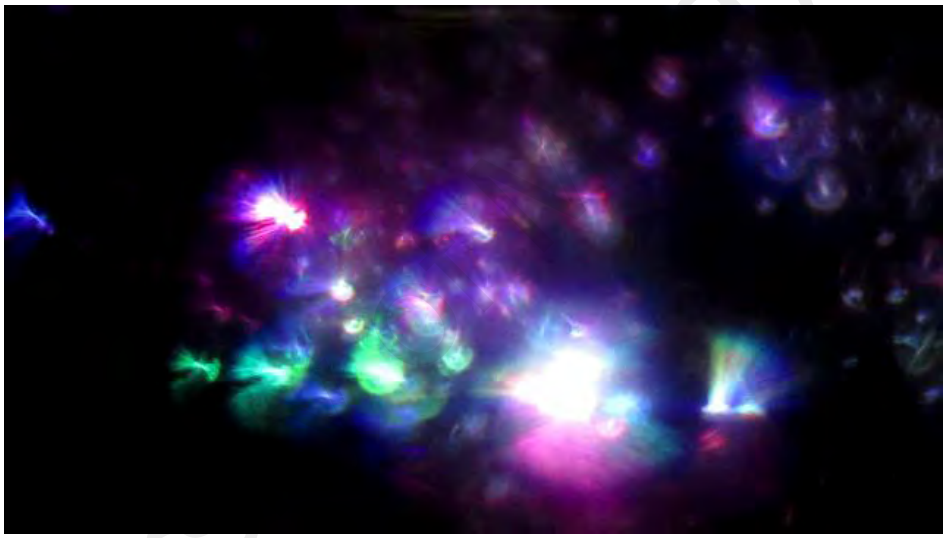

Time = 0.20 s

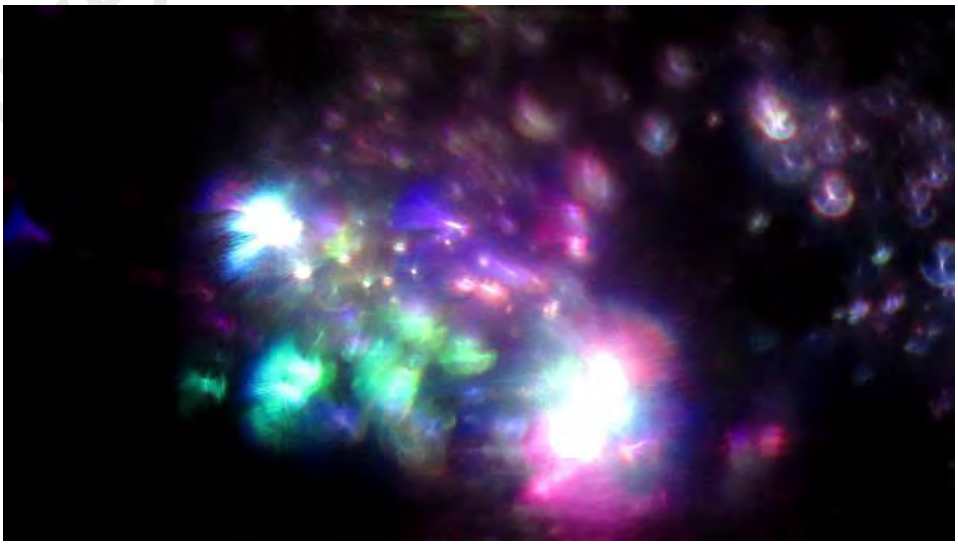

Time = 0.24 s

Figure 5.17, Continued.

As an additional information, Figure 5.17 has been added to demonstrate how focused region of laser inside water gets vibrant motion with sparkling colors with respect to time. Here no single bubble is visible because of non-focusing condition with the reason of no presence of halogen light (Figure 4.1). So, from these sequential pictures, we cannot track single or individual bubbles but can observe changeable complex dynamic movements of the whole region, discussion of this dynamic is not present project's main issue but it has been chosen to be considered as an extension of present work. So mentioning this segment is necessary to get a guideline for further research.

CHAPTER 6: CONCLUSION AND SCOPE OF FUTURE WORK

In our work, we have studied the light scattering of cavitation bubbles in water created by focused intense femtosecond laser pulses. Experimentally, we discover the striking colorful sparkling lights in the water, in addition to the supercontinuum generation of white light similar to that in fiber where the striking colorful sparkling light can be seen only when the laser intensity is sufficiently low.

It is necessary to mention that despite the fact that various models have been used to study the laser cavitation of bubbles, the colored emissions have never been observed or studied before. Most of the previous research tended to focus on creating of laser induced bubbles, their growth, and dynamics rather than investigating optical phenomena. This study is the first step on the way towards enhancing our understanding of strong optical scattering by laser induced bubbles inside water.

The newly found scattering of colored lights has a simple explanation and which is not due to whispering gallery effect (A whispering gallery is usually a circular, hemispherical, elliptical or ellipsoidal enclosure, in which wave can travel around the circumference, this traveling effect is called whispering gallery effect) where the light wave is guided by the bubble surface. The microbubbles scatter off sparkling lights in the optical range that are blueshifted from 800 nm superimpose to give the broadband whitelight spectrum. The effect is explained by nonlinear optical processes through intense laser interactions with water molecules. By studying the dynamics (by analyzing video clips) of the formation of microbubbles and light scattering we are now able to explain the phenomena of the colored sparkling lights as due to scattering from nonlinear processes of filamentation hot spots at the backside interface of the bubbles.

The sparkling lights with colors, observed only at low laser intensity, indicate that the filamentation hot spot at a particular spatial point contains spectral composition centered at a certain wavelength, giving a distinct color. And, to investigate further the spectral width and profile of the sparkling light with a particular color we need to capture its spectrum by using ultrafast camera system with high sensitivity and this is a significant challenge and beyond our present capability. Though, we observe white light when the intensity is increased. However, furthermore investigation should have done by using ultrafast camera system to revile more phenomena in microscale.

Results so far have been very promising not only in fundamental science but also in the field of application. The future works may focus on the comparison with other aqueous mediums, ultrafast dynamical evolution corresponding to light emitting effects of the laser induced bubbles and underwater cavitation generated by femtosecond laser pulses. In this research work we considered tightly focus femtosecond laser, however, the supercontinuum emission from tight focusing geometry was always higher than the loose focusing geometry inside water. So this new found effect can be investigated with less focus or semi focus environment.

This research could be a useful aid for decision makers those want to work in the field of laser matter interaction, and it could be a helpful aid for understanding optical behaviors of liquid under high intense femtosecond laser focused condition in the field of medical. We also think that our finding might be useful for photonics, ablation under water, nanoparticle fabrication and related studies, material characterization, micro and nano structuring, lithography, or even topics like underwater drilling using high intense lasers.

The results and explanation with huge scope of further investigation presented here provide insights and understanding of the optical phenomena involved in high intense

laser interaction with liquid and interfaces. The physical mechanism is interesting and relevant to micro and nano photonics.

Our result is encouraging for doing more theoretical work on this new found optical scattering. Mathematical formulation of this scattering could bring us to a new frontier of theoretical understanding of optical properties during light matter interaction.

REFERENCES

Buchwalow, I. B., and Böcker, W. (2010). *Immunohistochemistry: basics and methods.* Berlin: Springer Verlag.

Agayan, R. R., Gittes, F., Kopelman, R., & Schmidt, C. F. (2002). Optical trapping near resonance absorption. *Applied Optics, 41*(12), 2318-2327.

Akhatov, I., Lindau, O., Topolnikov, A., Mettin, R., Vakhitova, N., & Lauterborn, W. (2001). Collapse and rebound of a laser-induced cavitation bubble. *Physics of Fluids, 13*(10*)*, 2805-2819.

Akhatov, I., Vakhitova, N., Topolnikov, A., Zakirov, K., Wolfrum, B., Kurz, T. & Lauterborn, W. (2002). Dynamics of laser-induced cavitation bubbles. *Experimental Thermal and Fluid Science, 26*(6), 731-737.

Aközbek, N., Scalora, M., Bowden, C. M., & Chin, S. L. (2001). White-light continuum generation and filamentation during the propagation of ultra-short laser pulses in air. *Optics Communications, 191*(3), 353-362.

Amoruso, S., Bruzzese, R., Wang, X., Nedialkov, N. N., & Atanasov, P. A. (2007). Femtosecond laser ablation of nickel in vacuum. *Journal of Physics D: Applied Physics, 40*(2), 331.

Backus, S., Durfee III, C. G., Murnane, M. M., & Kapteyn, H. C. (1998). High power ultrafast lasers. *Review of scientific instruments, 69*(3), 1207-1223.

Barnes, P. A., & Rieckhoff, K. E. (1968). Laser induced underwater sparks. *Applied Physics Letters, 13*(8), 282-284.

Barnes, P. A., & Rieckhoff, K. E. (1968). Laser induced underwater sparks. *Applied Physics Letters, 13*(8), 282-284. .

Berthe, L., Fabbro, R., Peyre, P., & Bartnicki, E. (1999). Wavelength dependent of laser shock-wave generation in the water-confinement regime. *Journal of Applied Physics, 85*(11), 7552-7555.

Berthe, L., Fabbro, R., Peyre, P., Tollier, L., & Bartnicki, E. (1997). Shock waves from a water-confined laser-generated plasma. *Journal of Applied Physics, 82*(6), 2826-2832.

Berthe, L., Sollier, A., Peyre, P., Fabbro, R., & Bartnicki, E. (2000). The generation of laser shock waves in a water-confinement regime with 50 ns and 150 ns XeCl excimer laser pulses. *Journal of physics D: Applied physics, 33*(17), 2142.

Bloembergen, N. (1974). Laser-induced electric breakdown in solids. IEEE Journal of Quantum Electronics, 10(3), 375-386.

Brujan, E. A. (2008). Shock wave emission from laser-induced cavitation bubbles in polymer solutions. *Ultrasonics, 48*(5), 423-426.

Brujan, E. A., Ikeda, T., & Matsumoto, Y. (2008). On the pressure of cavitation bubbles. *Experimental Thermal and Fluid Science, 32*(5), 1188-1191.

Chen, J., Ng, J., Liu, S., & Lin, Z. (2009). Analytical calculation of axial optical force on a Rayleigh particle illuminated by Gaussian beams beyond the paraxial approximation. *Physical Review E, 80*(2), 026607.

Chen, X., Xu, R. Q., Shen, Z. H., Lu, J., & Ni, X. W. (2004). Optical investigation of cavitation erosion by laser-induced bubble collapse. Optics & Laser Technology, *36*(3), 197-203.

Cheriaux, G., & Chambaret, J. P. (2001). Ultra-short high-intensity laser pulse generation and amplification. *Measurement Science and Technology, 12*(11), 1769.

Chin, S. L. (2010). Femtosecond laser filamentation *(Vol. 55)*. New York: *Springer*.

Chin, S. L., & Lagacé, S. (1996). Generation of H 2, O 2, and H 2 O 2 from water by the use of intense femtosecond laser pulses and the possibility of laser sterilization. *Applied Optics, 35*(6), 907-911.

Chiou, P. Y., Wu, T. H., Park, S. Y., & Chen, Y. (2010). Pulse laser driven ultrafast micro and nanofluidics system. International Society for Optics and Photonics. *Biosensing III (pp. 77590Z-77590Z)*.

Costache, F., Kouteva-Arguirova, S., & Reif, J. (2004). Sub–damage–threshold femtosecond laser ablation from crystalline Si: surface nanostructures and phase transformation. *Applied Physics A, 79*(4-6), 1429-1432.

Couairon, A., & Mysyrowicz, A. (2007). Femtosecond filamentation in transparent media. *Physics Reports, 441*(2), 47-189.

Crisp, M. D., N. L. Boling, and G. Dubé. (1972) Importance of Fresnel reflections in laser surface damage of transparent dielectrics. *Applied Physics Letters 21.8*, 364-366.

Csuka, Z., Olšiak, R., & Fuszko, Z. (2016). Research of Cavitation at High Shear Stress. Strojnícky casopis. J*ournal of Mechanical Engineering, 66*(1), 7-16.

DeMichelis, C. (1969). Laser induced gas breakdown: A bibliographical review. IEEE *Journal of Quantum Electronics, 5*(4), 188-202.

Devaux, D., Fabbro, R., Tollier, L., & Bartnicki, E. (1993). Generation of shock waves by laser-induced plasma in confined geometry. *Journal of Applied Physics, 74*(4), 2268-2273.

Docchio, F., Regondi, P., Capon, M. R., & Mellerio, J. (1988). Study of the temporal and spatial dynamics of plasmas induced in liquids by nanosecond Nd: YAG laser pulses. 1: Analysis of the plasma starting times. *Applied Optics, 27*(17), 3661-3668.

Doukas, A. G., Zweig, A. D., Frisoli, J. K., Birngruber, R., & Deutsch, T. F. (1991). Non-invasive determination of shock wave pressure generated by optical breakdown. Applied Physics B: *Lasers and Optics, 53*(4), 237-245.

E. Hecht, (1987), Optics, Addison-Wesley, Reading, MA, 2nd edn.

Felix, M. P., & Ellis, A. T. (1971). Laser-Induced Liquid Breakdown-a Step-By-Step Account. *Applied Physics Letters, 19*(11), 484-486.

Feng, Q., Wright, E. M., Moloney, J. V., & Newell, A. C. (1995). Laser-induced breakdown versus self-focusing for focused picosecond pulses in water. *Optics Letters, 20(19)*, 1958-1960.

Grand, D., Bernas, A., & Amouyal, E. (1979). Photoionization of aqueous indole: Conduction band edge and energy gap in liquid water. *Chemical Physics, 44*(1), 73-79.

Hammer, D. X., Jansen, E. D., Frenz, M., Noojin, G. D., Thomas, R. J., Noack, J., & Welch, A. J. (1997). Shielding properties of laser-induced breakdown in water for pulse durations from 5 ns to 125 fs. *Applied Optics, 36*(22), 5630-5640.

Hao, Z., Stelmaszczyk, K., Rohwetter, P., Nakaema, W. M., & Woeste, L. (2011). Femtosecond laser filament-fringes in fused silica. *Optics Express, 19*(8), 7799-7806.

Herd, R. M., Dover, J. S., & Arndt, K. A. (1997). Basic laser principles. *Dermatologic Clinics, 15*(3), 355-372.

Hickling, R., & Plesset, M. S. (1964). Collapse and rebound of a spherical bubble in water. *The Physics of Fluids, 7*(1), 7-14.

Hitz, C. B., Ewing, J. J., & Hecht, J. (2012). Introduction to laser technology. John Wiley & Sons.

Ilyin, A. A., & Golik, S. S. (2013). Femtosecond laser-induced breakdown spectroscopy of sea water. *Spectrochimica Acta Part B: Atomic Spectroscopy, 87*, 192-197.

Juhasz, T., Hu, X. H., Turi, L., & Bor, Z. (1994). Dynamics of shock waves and cavitation bubbles generated by picosecond laser pulses in corneal tissue and water. *Lasers in Surgery and Medicine, 15*(1), 91-98.ds

Juhasz, T., Pho, G. A. K., Bs, C. S., Ms, Z. B., & Bron, W. E. (1996). Time-Resolved Observations of Shock Waves and Cavitation Bubbles Generated. *Lasers in Surgery and Medicine, 19*, 23-31.

Kabashin, A. V., Meunier, M., Kingston, C., & Luong, J. H. (2003). Fabrication and characterization of gold nanoparticles by femtosecond laser ablation in an aqueous solution of cyclodextrins. *The Journal of Physical Chemistry B, 107*(19), 4527-4531.

Kaiser, W., & Auston, D. H. (Eds.). (1993). Ultrashort Laser Pulses: Generation and Applications. *Springer*.

Kaltz, E.L. (1986), The stability of turbidity in raw water and its relationship to chlorine demand. *Journal of American Water Works Association. 78*, 72 – 75

Kamlage, G., Bauer, T., Ostendorf, A., & Chichkov, B. N. (2003). Deep drilling of metals by femtosecond laser pulses. *Applied Physics A, 77*(2), 307-310.

Kennedy, P. K., Hammer, D. X., & Rockwell, B. A. (1997). Laser-induced breakdown in aqueous media. *Progress in Quantum Electronics, 21(3)*, 155-248.

Kennedy, P. K. (1995). A first-order model for computation of laser-induced breakdown thresholds in ocular and aqueous media. I. Theory. *IEEE Journal of Quantum Electronics, 31*(12), 2241-2249.

Kim, D., Park, H. K., & Grigoropoulos, C. P. (2001). Interferometric probing of rapid vaporization at a solid–liquid interface induced by pulsed-laser irradiation. *International Journal of Heat and Mass Transfer, 44*(20), 3843-3853.

Kiran, P. P., Bagchi, S., Krishnan, S. R., Arnold, C. L., Kumar, G. R., & Couairon, A. (2010). Focal dynamics of multiple filaments: Microscopic imaging and reconstruction. *Physical Review A, 82*(1), 013805.

Kosareva, O. G., Kandidov, V. P., Brodeur, A., Chien, C. Y., & Chin, S. L. (1997). Conical emission from laser–plasma interactions in the filamentation of powerful ultrashort laser pulses in air. *Optics Letters, 22*(17), 1332-1334.

Kruusing, A. (2004). Underwater and water-assisted laser processing: part 1—general features, steam cleaning and shock processing. *Optics and Lasers in Engineering, 41*(2), 307-327.

Kruusing, A. (2004). Underwater and water-assisted laser processing: Part 2—Etching, cutting and rarely used methods. *Optics and Lasers in Engineering, 41*(2), 329-352.

Lenzner, M., Spielmann, C., Wintner, E., Krausz, F., & Schmidt, A. J. (1995). Sub-20-fs, kilohertz-repetition-rate Ti: sapphire amplifier. *Optics Letters, 20*(12), 1397-1399.

Lim, K. Y., Quinto-Su, P. A., Klaseboer, E., Khoo, B. C., Venugopalan, V., & Ohl, C. D. (2010). Nonspherical laser-induced cavitation bubbles. *Physical Review E, 81*(1), 016308.

Lindau, O., & Lauterborn, W. (2003). Cinematographic observation of the collapse and rebound of a laser-produced cavitation bubble near a wall. *Journal of Fluid Mechanics, 479*, 327-348.

Liu, F., Yuan, S., Zuo, Z., Li, W., & Zeng, H. (2016). Laser filamentation induced bubbles and their motion in water. *Optics Express, 24*(12), 13258-13263.

Liu, W., Kosareva, O., Golubtsov, I. S., Iwasaki, A., Becker, A., Kandidov, V. P., & Chin, S. L. (2003). Femtosecond laser pulse filamentation versus optical breakdown in H 2 O. *Applied Physics B: Lasers and Optics, 76*(3), 215-229.

Liu, X., Du, D., & Mourou, G. (1997). Laser ablation and micromachining with ultrashort laser pulses. *IEEE Journal of Quantum Electronics, 33*(10), 1706-1716.

Loesel, F. H., Fischer, J. P., Götz, M. H., Horvath, C., Juhasz, T., Noack, F., & Bille, J. F. (1998). Non-thermal ablation of neural tissue with femtosecond laser pulses. *Applied Physics B: Lasers and Optics, 66*(1), 121-128.

Machmudah, S., Kuwahara, Y., Sasaki, M., & Goto, M. (2011). Nano-structured particles production using pulsed laser ablation of gold plate in supercritical CO^2. *The Journal of Supercritical Fluids, 60*, 63-68.

Marburger, J. H. (1975). Self-focusing: theory. *Progress in Quantum Electronics, 4*, 35-110.

Mizushima, Y., & Saito, T. (2015). Nonlinear bubble nucleation and growth following filament and white-light continuum generation induced by a single-shot femtosecond laser pulse into dielectrics based on consideration of the time scale. *Applied Physics Letters, 107*(11), 114102.

Noack, J., & Vogel, A. (1999). Laser-induced plasma formation in water at nanosecond to femtosecond time scales: calculation of thresholds, absorption coefficients, and energy density. *IEEE Journal of Quantum Electronics, 35*(8), 1156-1167.

O. Zvelto (2004). Principles of lasers, Plenum, NY

Ohl, C. D., Kurz, T., Geisler, R., Lindau, O., & Lauterborn, W. (1999). Bubble dynamics, shock waves and sonoluminescence. Philosophical Transactions of the Royal Society of London A: Mathematical, *Physical and Engineering Sciences, 357*(1751), 269-294.

Ong, C., Ibrahim, S., & Sen Gupta, B. (2007). A survey of tap water quality in Kuala Lumpur. *Urban Water Journal, 4(1)*, 29-41.

Ooi, C. R., & Talib, M. R. (2016). Intricate plasma-scattered images and spectra of focused femtosecond laser pulses. *Scientific Reports, 6*, 32056.

Ooi, C. R., & Sanny, A.I. (2017). Multispectral sparkling of microbubbles with a focused femtosecond laser, *Journal of the Optical Society of America B 34*(10), 2072-2080

Park, H. K., Grigoropoulos, C. P., Poon, C. C., & Tam, A. C. (1996). Optical probing of the temperature transients during pulsed-laser induced boiling of liquids. *Applied Physics Letters, 68*(5), 596-598.

Park, H. K., Kim, D., Grigoropoulos, C. P., & Tam, A. C. (1996). Pressure generation and measurement in the rapid vaporization of water on a pulsed-laser-heated surface. *Journal of Applied Physics, 80*(7), 4072-4081.

Park, H. K., Zhang, X., Grigoropoulos, C. P., Poon, C. C., & Tam, A. C. (1996). Transient temperature during the vaporization of liquid on a pulsed laser-heated solid surface. *Journal of Heat Transfer, 118*(3), 702-708.

Patterson, F. G., Perry, M. D., Gonzales, R., & Campbell, E. M. (1990). Multiterawatt Nd: glass lasers based on chirped-pulse amplification. In Femtosecond to Nanosecond High-Intensity Lasers and Applications (Vol. 1229, pp. 2-19). International Society for Optics and Photonics.

Perelomov, A. M., Popov, V. S., & Terent'ev, M. V. (1966). Ionization of atoms in an alternating electric field. *Soviet Physics JETP, 23*(5), 924-934.

Peyre, P., & Fabbro, R. (1995). Laser shock processing: a review of the physics and applications. *Optical and Quantum Electronics, 27*(12), 1213-1229.

Peyre, P., Berthe, L., Scherpereel, X., & Fabbro, R. (1998). Laser-shock processing of aluminium-coated 55C1 steel in water-confinement regime, characterization and application to high-cycle fatigue behaviour. *Journal of Materials Science, 33*(6), 1421-1429.

Potemkin, F. V., Mareev, E. I., Podshivalov, A. A., & Gordienko, V. M. (2014). Laser control of filament-induced shock wave in water. *Laser Physics Letters, 11*(10), 106001.

Putterman, S. J., & Weninger, K. R. (2000). Sonoluminescence: How bubbles turn sound into light. *Annual Review of Fluid Mechanics, 32*(1), 445-476.

Rastopov, S. F., & Sukhodol'sky, A. T. (1990). Cluster nucleation in the process of CW laser induced thermocavitation. *Physics Letters A, 149*(4), 229-232.

Sacchi, C. A. (1991). Laser-induced electric breakdown in water. *Journal of the Optical Society of America B, 8*(2), 337-345.

Sakakura, M., Terazima, M., Shimotsuma, Y., Miura, K., & Hirao, K. (2007). Observation of pressure wave generated by focusing a femtosecond laser pulse inside a glass. *Optics Express, 15*(9), 5674-5686.

Sankin, G. N., Simmons, W. N., Zhu, S. L., & Zhong, P. (2005). Shock wave interaction with laser-generated single bubbles. *Physical Review Letters, 95*(3), 034501

Sankin, G. N., Simmons, W. N., Zhu, S. L., & Zhong, P. (2005). Shock wave interaction with laser-generated single bubbles. *Physical Review Letters, 95*(3), 034501.

Schaffer, C., Nishimura, N., Glezer, E., Kim, A., & Mazur, E. (2002). Dynamics of femtosecond laser-induced breakdown in water from femtoseconds to microseconds. *Optics Express, 10*(3), 196-203.

Shen, M. Y., Crouch, C. H., Carey, J. E., & Mazur, E. (2004). Femtosecond laser-induced formation of submicrometer spikes on silicon in water. *Applied Physics Letters, 85*(23), 5694-5696.

Shen, N., Datta, D., Schaffer, C. B., LeDuc, P., Ingber, D. E., & Mazur, E. (2005). Ablation of cytoskeletal filaments and mitochondria in live cells using a femtosecond laser nanoscissor. *Mechanics & Chemistry of Biosystems, 2*(1), 17-25.

Silfvast, W. T. (2004). Laser Fundamentals. Cambridge University Press.

Soileau, M. J., Williams, W. E., Mansour, N., & Van Stryland, E. W. (1989). Laser-induced damage and the role of self-focusing. *Optical Engineering, 28*(10), 281133-281133.

Sollier, A., Berthe, L., & Fabbro, R. (2001). Numerical modeling of the transmission of breakdown plasma generated in water during laser shock processing. *The European Physical Journal Applied Physics, 16*(2), 131-139.

Sreeja, S., Leela, C., Kumar, V. R., Bagchi, S., Prashant, T. S., Radhakrishnan, P., & Kiran, P. P. (2013). Dynamics of tightly focused femtosecond laser pulses in water. *Laser Physics, 23*(10), 106002.

Sugioka, K., & Cheng, Y. (2014). Ultrafast lasers—reliable tools for advanced materials processing. *Light: Science & Applications, 3*(4), e149.

Sullivan, A., Hamster, H., Kapteyn, H. C., Gordon, S., White, W., Nathel, H., & Falcone, R. W. (1991). Multiterawatt, 100-fs laser. *Optics letters, 16*(18), 1406-1408.

Sutter, D. H., Jung, I. D., Kartner, F. X., Matuschek, N., Morier-Genoud, F., Scheuer, V., & Keller, U. (1998). Self-starting 6.5-fs pulses from a Ti: sapphire laser using a semiconductor saturable absorber and double chirped mirrors. *IEEE Journal of Selected Topics in Quantum Electronics, 4*(2), 169-178.

Unger, B. T., & Marston, P. L. (1988). Optical levitation of bubbles in water by the radiation pressure of a laser beam: an acoustically quiet levitator. *The Journal of the Acoustical Society of America, 83*(3), 970-975.

Vogel, A., Busch, S., Jungnickel, K., & Birngruber, R. (1994). Mechanisms of intraocular photodisruption with picosecond and nanosecond laser pulses. *Lasers in Surgery and Medicine, 15*(1), 32-43.

Vogel, A., Engelhardt, R., Behnle, U., & Parlitz, U. (1996). Minimization of cavitation effects in pulsed laser ablation illustrated on laser angioplasty. *Applied Physics B: Lasers and Optics, 62*(2), 173-182.

Vogel, A., Lauterborn, W., & Timm, R. (1989). Optical and acoustic investigations of the dynamics of laser-produced cavitation bubbles near a solid boundary. *Journal of Fluid Mechanics, 206*, 299-338.16.

Vogel, A., Noack, J., Nahen, K., Theisen, D., Busch, S., Parlitz, U., & Birngruber, R. (1999). Energy balance of optical breakdown in water at nanosecond to femtosecond time scales. *Applied Physics B: Lasers and Optics, 68*(2), 271-280.

Williams, D. (2008). Laser basics. Anaesthesia & Intensive Care Medicine, 9(12), 550-552.

Womack, M., Vendan, M., & Molian, P. (2004). Femtosecond pulsed laser ablation and deposition of thin films of polytetrafluoroethylene. *Applied Surface Science, 221*(1), 99-109.

Wright, W. H., Sonek, G. J., & Berns, M. W. (1994). Parametric study of the forces on microspheres held by optical tweezers. *Applied Optics, 33*(9), 1735-1748.

Xu, Z., Zhu, X., Yu, Y., Zhang, N., & Zhao, J. (2014). Super-luminescent jet light generated by femtosecond laser pulses. *Scientific Reports, 4*. 3892

Yang, G. W. (2007). Laser ablation in liquids: applications in the synthesis of nanocrystals. *Progress in Materials Science, 52*(4), 648-698.

Yavas, O., Leiderer, P., Park, H. K., Grigoropoulos, C. P., Poon, C. C., & Tam, A. C. (1994). Enhanced acoustic cavitation following laser-induced bubble formation: Long-term memory effect. *Physical Review Letters, 72*(13), 2021.

Yavas, O., Leiderer, P., Park, H. K., Grigoropoulos, C. P., Poon, C. C., Leung, W. P. & Tam, A. C. (1994). Optical and acoustic study of nucleation and growth of bubbles at a liquid-solid interface induced by nanosecond-pulsed-laser heating. *Applied Physics A, 58*(4), 407-415.

Z. Chen, A. Taflove, and V. Backman, (2004). Photonic nanojet enhancement of backscattering of light by nanoparticles: a potential novel visiblelight ultramicroscopy technique, *Optical Express 12*, 1214–1220.

Zysset, B., Fujimoto, J. G., & Deutsch, T. F. (1989). Time-resolved measurements of picosecond optical breakdown. *Applied Physics B, 48*(2), 139-147.

LIST OF PUBLICATIONS AND PAPERS PRESENTED

This work has been published on the date 8th September 2017, publication details :

Ooi & **Sanny**, (2017). Multispectral sparkling of microbubbles with a focused femtosecond laser, *Journal of the Optical Society of America* B, *34* (10), 2072-2080.